technologies

MDPI

Review

Enhancing the Performance of Materials in Ballistic Protection Using Coatings—A Review

Georgiana Ghisman Alexe [1], Gabriel Bogdan Carp [1], Tudor Viorel Tiganescu [2,*] and Daniela Laura Buruiana [1,*]

[1] Interdisciplinary Research Centre in the Field of Eco-Nano Technology and Advance Materials CC-ITI, Faculty of Engineering, "Dunarea de Jos" University of Galati, 47 Domneasca, 800008 Galati, Romania; georgiana.ghisman@ugal.ro (G.G.A.); gabriel.carp@ugal.ro (G.B.C.)
[2] Military Technical Academy "Ferdinand I", 39-49 George Cosbuc Boulevard, 050141 Bucharest, Romania
* Correspondence: tiganescu.tvt@gmail.com (T.V.T.); daniela.buruiana@ugal.ro (D.L.B.)

Abstract

The continuous advancement of modern weaponry has intensified the pursuit of next-generation ballistic protection systems that integrate lightweight architectures, superior flexibility, and high energy absorption efficiency. This review provides a technological overview of current trends in the design, processing, and performance optimization of metallic, ceramic, polymeric, and composite materials for ballistic applications. Particular emphasis is placed on the role of advanced surface coatings and nanostructured interfaces as enabling technologies for improved impact resistance and multifunctionality. Conventional materials such as high-strength steels, alumina, silicon carbide, boron carbide, Kevlar®, and ultra-high-molecular-weight polyethylene (UHMWPE) continue to dominate the field due to their outstanding mechanical properties; however, their intrinsic limitations have prompted a transition toward nanotechnology-assisted solutions. Functional coatings incorporating nanosilica, graphene and graphene oxide, carbon nanotubes (CNTs), and zinc oxide nanowires (ZnO NWs) have demonstrated significant enhancement in interfacial adhesion, inter-yarn friction, and energy dissipation. Moreover, multifunctional coatings such as CNT- and laser-induced graphene (LIG)-based layers integrate sensing capability, electromagnetic interference (EMI) shielding, and thermal stability, supporting the development of smart and adaptive protection platforms. By combining experimental evidence with computational modeling and materials informatics, this review highlights the technological impact of coating-assisted strategies in the evolution of lightweight, high-performance, and multifunctional ballistic armor systems for defense and civil protection.

Keywords: surface coatings; nanomaterials; nanotechnologies; energy absorption; lightweight body armor

Check for updates

Academic Editors: Manoj Gupta and Zhixing Guo

Received: 16 October 2025
Revised: 4 December 2025
Accepted: 20 December 2025
Published: 24 December 2025

Copyright: © 2025 by the authors. Licensee MDPI, Basel, Switzerland. This article is an open access article distributed under the terms and conditions of the Creative Commons Attribution (CC BY) license.

1. Introduction

The protection of the human body against various types of physical threats, such as sharp objects, projectiles, or other forms of impact, dates back to ancient times, when the instinct for survival led people to seek defense methods using materials such as leather, wood, stone, copper, or steel [1]. Gradually, steel plate armors were developed, arranged in a way that covered vital areas, later evolving into combined layers of silk, rubber, and steel [2]. However, over time, the growing need for protection against new types of weapons led to the refinement of protective equipment and the emergence of advanced armor made of metals and ceramics, recognized for their bullet-resistant properties [3].

Nevertheless, due to their rigidity, these materials could not provide effective protection for areas such as joints, the neck, or the shoulders [4]. Therefore, the development of advanced ballistic protection systems is necessary, characterized by high impact resistance, flexibility, reduced weight, and excellent energy absorption capacity, while also ensuring comfort in response to the demands of modern military operations, technology-based warfare tactics, and the weapons and ammunition currently in use [5].

At present, the defense industry, in collaboration with researchers in the field of materials science, is focusing on the development and improvement of protection systems designed for military equipment and personnel, with the aim of enhancing their performance under complex operational conditions and increasing resistance against threats encountered in combat operations [6]. These research efforts have led to the development of high-performance fibers with diverse structures and properties, capable of providing specific responses to impact, both at the filament level and in the form of woven fabrics or composite laminates [7]. Among them, para-aramids and ultra-high-molecular-weight polyethylene (UHMWPE) represent some of the most widely used high-performance fibers in ballistic protection textiles due to their exceptional impact resistance [8]. Notable examples include Twaron—a registered trademark of Teijin, Kevlar—a registered trademark of DuPont, Dyneema—a registered trademark of DSM, and Spectra—a registered trademark of Honeywell, all of which are internationally recognized for their superior performance. These fibers are extensively employed in the design of flexible ballistic protection vests, owing to their key engineering characteristics—high mechanical strength, excellent toughness, good chemical resistance, and low weight—all of which contribute to the efficiency and comfort of personal protective equipment [7]. In general, in order to ensure superior resistance against different types of ballistic impacts, the aforementioned high-performance fibers must be modified at various stages of use, whether in the form of filaments, fabrics, or the corresponding textile composite reinforcement materials [9,10]. For numerous applications, such as vests or their components, the fibers are commonly employed in the form of woven or knitted fabrics [11]. In addition to the intrinsic properties of the materials, improving the ballistic performance of composite panels requires considering mechanisms such as increasing the number of layers and arranging them in specific stacking configurations. Previous studies have shown that energy absorption efficiency is strongly influenced by the multilayer architecture: Yang and Chen [12] demonstrated the contribution of layer interactions to energy dissipation in soft armor; Zohdi [13] and Joo and Kang [14] highlighted, through numerical modeling, how progressive penetration and inter-ply dynamics depend on ply arrangement; Karahan et al. [15] reported that woven aramid fabrics exhibit different ballistic responses depending on fabric layering; and Liu et al. [16] showed that increasing the number of layers or introducing air gaps can significantly alter ballistic resistance. However, although these strategies enhance protection, they may also negatively affect the overall weight and flexibility of the panel. Coatings applied to materials used in ballistic protection represent an innovative solution for enhancing their performance, as they can simultaneously contribute to improving impact resistance, optimizing the absorption and dissipation of kinetic energy, and protecting the substrate against wear, abrasion, or chemical degradation. By tailoring the thickness, composition, and microstructure of the deposited layer, these coatings not only increase the mechanical efficiency of the base material but also extend the service life of protective equipment, providing an additional barrier against extreme operating conditions. Furthermore, the role of coating has become increasingly important in the context of reducing the weight of ballistic protection systems, since they enable an optimal balance between mass and performance by integrating multiple functionalities into a thin and efficient layer. They can be designed to impart characteristics such as hydrophobicity, high-temperature resistance, compatibility with

polymeric or ceramic materials, and even self-healing capabilities, thereby contributing to the development of advanced ballistic vests and panels that meet modern requirements of security, mobility, and comfort.

In the context of this review, ballistic protection is discussed with direct reference to the key material components used in soft and hard armor systems, namely, high-performance fibers such as Kevlar®, Twaron®, Dyneema®, and Spectra®, typically employed in the form of woven fabric layers or composite laminates. These substrates represent the structural core of helmets, soft ballistic vests, trauma plates, and hybrid protective panels. The coatings examined in this article, such as shear-thickening fluids (STFs), ceramic and silica nanoparticles, graphene-based layers, carbon nanotube (CNT) treatments, and hydrothermally grown ZnO nanostructures, are applied directly onto these fibers and fabric systems to improve their response to ballistic impact by enhancing inter-yarn friction, stiffness, energy absorption, and resistance to penetration. This review specifically focuses on these coated fiber-based components and their functional role in ballistic impact mitigation.

Despite significant advances in high-performance fibers, ceramics, and hybrid armor systems, a critical research gap remains achieving an optimal balance between flexibility and lightweight design, which is essential for user mobility and sufficient resistance to penetrating impact. Conventional approaches often improve ballistic resistance at the expense of panel deformability or weight, revealing the need for new material architectures and surface-engineering strategies capable of enhancing energy absorption without compromising flexibility. The technologies reviewed in this work address precisely this tradeoff by focusing on micro- and nanoscale coatings, structural tuning, and hybrid interfaces that strengthen fiber–fiber interactions while maintaining low areal density.

The main purpose of this review article is to provide a comprehensive analysis of the performance of materials and coatings applied to those used in ballistic protection, with an emphasis on the mechanisms through which they contribute to enhancing mechanical properties, impact resistance, and durability. This paper explores different types of coatings, deposition technologies, and their influence on the behavior of base materials in the context of current demands for more efficient, lighter, and better energy-absorbing ballistic protective equipment.

2. Materials for Ballistic Protection

Modern materials used in the ballistic protection of humans and vehicles must be lightweight, with low density, while at the same time strong, hard, durable, and capable of stopping or fragmenting projectiles of certain calibers. They are generally classified into four main categories, metals, ceramics, polymers, and composites [17], as can be seen in Figure 1.

Ballistic performance is typically evaluated according to internationally recognized standards. The most widely adopted being the National Institute of Justice (NIJ) standard and the NATO STANAG specifications. The NIJ 0101.06/0101.07 [18] standards classify ballistic threats into protection levels based on projectile type, velocity, and impact energy and require both perforation resistance and back-face signature (BFS) measurements. BFS quantifies the depth of the indentation left on a calibrated clay backing material and is used to assess blunt trauma risk. The standard also prescribes strict environmental conditioning, shot placement rules, and multi-hit requirements to ensure consistent evaluation.

Similarly, NATO STANAG 4569 [19] and related Allied Engineering Publications (AEP-55) define ballistic protection levels for military vehicles and personal armor, specifying projectile caliber, impact velocity, stand-off distance, and acceptable penetration criteria. Unlike NIJ, STANAG tests focus primarily on complete perforation assessment and platform survivability rather than BFS. The standard also includes V50 ballistic limit

testing the velocity at which 50% of projectiles penetrate, providing a statistically robust measure of material performance.

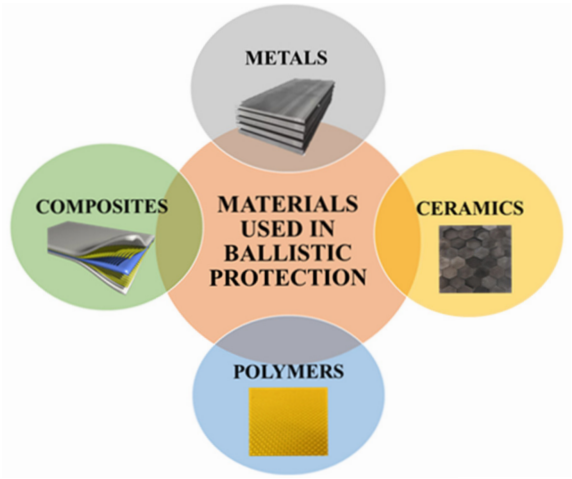


Figure 1. Classification of materials used in ballistic protection.

Together, NIJ and STANAG methodologies offer complementary frameworks for evaluating the effectiveness of armor systems. While NIJ emphasizes personal protection and blunt trauma mitigation, STANAG focuses on military-grade ballistic threats and structural integrity. Including both perspectives allows a more holistic assessment of how coatings, hybrid architectures, and fiber-reinforced systems improve resistance under varied operational conditions.

2.1. Metals

Metals are among the earliest materials used for ballistic armor, valued for their inherent strength and durability [20]. High-strength steels, such as Armox 500T, Hardox 450, and PROTAC 500, are preferred in ballistic applications due to their remarkable balance between mechanical strength and toughness, enabling efficient absorption and dispersion of impact energy, as demonstrated in numerous experimental studies and microstructural analyses [21–24].

Next-generation armor steels undergo advanced thermo-mechanical processing and specialized alloying, which can achieve strength values approximately several thousand MPa, thereby substantially contributing to weight reduction in structures without compromising ballistic protection. Hardox 450 steel stands out in both civilian and military applications not only for its hardness and abrasion resistance but also for its superior ductility and toughness, which are achieved through a combination of optimized alloy composition, controlled quenching, and tempering processes. These thermo-mechanical treatments refine the microstructure and ensure a balanced performance, making Hardox 450 suitable for ballistic barriers in shooting ranges [24]. A recent study by Vilis et al. [25] demonstrated that the integration of a thin Hardox 450 steel layer, 2 mm in thickness, inserted between advanced textile composite layers (Twaron CT747 and Endumax Shield XF33) provides effective ballistic protection against 7.62 mm FMJ M80 projectiles (~830 m/s), successfully stopping the impact without penetration, achieving an optimal balance between reduced weight and high ballistic performance, as confirmed by subsequent analyses showing that hybrid metal–composite configurations can reach areal densities as low as 68.6 kg/m^2 (with a 4 mm steel layer) while still meeting STANAG 4569 Level 1 requirements, benefiting from the synergistic interaction between the steel front layer and the energy-absorbing textile composites, and validated through both experimental testing and numerical simulations. Furthermore, Acar et al. [26] investigated the ballistic

performance of Armox Advance, Ramor 500, and Hardox 450 steels in different thicknesses and configurations (monolithic, double-layered, and reperforated) against 7.62 mm and 12.7 mm projectiles. Their results showed that although Hardox 450 alone does not provide complete ballistic protection, it is effective when used as a sacrificial layer in combination with Armox Advance plates, thereby enhancing the resistance of layered systems.

2.2. Ceramics

Ceramic materials are recognized as highly effective for use in ballistic protection [27,28], primarily due to their properties, such as high hardness, stiffness, resistance to elevated temperatures, and environmental stability. These characteristics arise from their chemical structure, which is dominated by strong atomic bonds that prevent relative atomic displacement. However, the greatest advantage of ceramics remains their low areal density, combined with the ability to fracture hard-core projectiles, making them extremely effective in stopping high-energy bullets [29].

The most widely used ceramic materials in modern armor systems are Al_2O_3 (alumina), SiC (silicon carbide), and B_4C (boron carbide) [30]. Their selection depends on a balance between cost, mechanical toughness, manufacturability, and ballistic efficiency, as each ceramic exhibits distinct advantages. Alumina is preferred for its low cost and good manufacturability, despite its higher density. Under ballistic impact, alumina typically fails through a conical cracking and shear-plugging mechanism, producing granular fragmentation. Analytical and geometric models describing these processes enable optimized plate configuration and thickness design, ensuring sufficient protection while reducing system mass [31,32].

Silicon carbide (SiC) occupies an intermediate position between alumina and boron carbide. It combines lower density with higher hardness and fracture strength compared to alumina, providing ballistic performance close to B_4C but at a considerably lower cost [33]. Boron carbide exhibits the highest ballistic efficiency among ceramic armor materials due to its extremely low density and very high hardness. However, its performance is limited by stress-induced amorphization that occurs under high shock or shear loading, a mechanism that significantly reduces shear strength and decreases ballistic resistance. Consequently, the material's effectiveness strongly depends on controlling amorphization through the careful tuning of composition and microstructure, while its manufacturing and processing costs remain substantially higher than those of alumina and SiC [34,35].

Recent work by Yemao He et al. [36] demonstrated that the ballistic efficiency of SiC-based composite panels can be markedly improved by optimizing the mass ratio between the ceramic front layer and the backing plate. A ratio of approximately 72/28 (front/back) was shown to provide superior resistance against full-velocity impacts from 7.62 mm and 12.7 mm API projectiles by enabling efficient projectile erosion while ensuring effective stabilization and energy absorption by the backing. Additional improvements were achieved through square mosaic geometries and 3D confinement structures, which reduced damage spread and enhanced multi-hit capability.

The influence of composition on SiC ceramics has also been investigated by Jeremias Ismael Nunes Fortini et al. [31], who examined the effect of silicon additions. Increasing silicon content reduced relative density and mechanical strength due to higher porosity and decreased flexural properties; however, all compositions still met the NIJ 0123.00 RF2 [37] ballistic requirements, maintaining BFS values below the 44 mm limit. Low-silicon compositions (0–5%) provided the best mechanical integrity, while higher silicon levels (15–25%) resulted in significantly reduced density, making them attractive for lightweight armor applications when a mass reduction was prioritized.

Boron carbide (B_4C) offers the highest ballistic efficiency among the three ceramics because of its extremely low density and very high hardness. Its main limitation is stress-induced amorphization during high shock or shear loading, which decreases shear strength and negatively affects ballistic performance. Therefore, its practical efficiency strongly depends on controlling composition and microstructure to mitigate amorphization effects [34,35]. Temperature further affects B_4C behavior: Dongfang Xu et al. [38] showed that B_4C-based composite panels perform significantly better at sub-zero temperatures (−40 °C), where higher hardness and reduced radial crack propagation enhance projectile erosion. In contrast, elevated temperatures (+70 °C) lead to extensive radial cracking, increased deformation of the backing plate, and overall reduced protective capability. These temperature-dependent mechanisms highlight the importance of environmental conditions in the design of lightweight armor systems based on B_4C. B_4C ceramics, when employed as the outer layer of a bulletproof vest, provide remarkable protection against armor-piercing incendiary projectiles, especially when combined with a suitable composite backing [39]. The use of functionally graded materials (FGMs), such as B_4C/Al plates with a linear composition gradient along the thickness, has shown optimal ballistic resistance in testing, demonstrating that material gradation plays a decisive role in bulletproof protection [40].

2.3. Polymeric Materials

Polymers, recognized for their low weight and flexibility, provide significant advantages in the field of ballistic protection. Aramid and polyethylene fibers are frequently used in armor systems due to their low density, ensuring high mobility without compromising the level of protection [41], as their reduced mass (1.44 g/cm^3 for aramid and ~0.97 g/cm^3 for UHMWPE) allows the incorporation of multiple energy-absorbing layers without a substantial weight penalty. In addition to low density, these fibers exhibit high tensile strength, large failure strain, and efficient in-plane energy distribution through fibrillation and fiber stretching, which together enhance the armor's ability to dissipate the kinetic energy of the projectile. Currently, commercial bulletproof vests mainly employ two types of polymeric fibers:

- Para-aramid (e.g., Kevlar, Twaron, Technora);
- Ultra-high-molecular-weight polyethylene (UHMWPE) [42].

Kevlar began to be used in the manufacturing of bulletproof vests in the mid-1970s, with the first fully developed vest produced in 1976, only a few years after its discovery by Stephanie Kwolek in 1971 [43]. This innovation significantly reduced the overall weight of bulletproof vests and improved the mobility of the wearer, leading to the development of the modern vests used today.

Kevlar is a synthetic fiber belonging to the class of aromatic polymers, recognized for its exceptional properties and its unique chemical composition based on aromatic polyamides (aramids). These characteristics clearly distinguish it from other artificial fibers, owing to its very high mechanical strength, high elastic modulus, low weight, and excellent chemical stability. In addition, Kevlar is notable for its ability to limit thermal expansion, maintain dimensional stability, and exhibit pronounced rigidity [44].

Through the polymerization process, synthetic fibers are obtained which, when woven, form Kevlar—a high-strength material valued for its high strength-to-weight ratio, being approximately five times stronger than steel on an equal weight basis [45].

One intensively explored area of research concerning the impact resistance of Kevlar focuses on analyzing the influence of shear-thickening fluids (STFs) on the ballistic performance of Kevlar-reinforced composites [46–50].

A shear-thickening fluid (STF) is a non-Newtonian suspension whose viscosity increases as the external shear rate or applied stress intensifies [51,52]. Owing to this property,

Kevlar fabrics impregnated with STFs are increasingly employed in ballistic protection, offering an optimal balance between the comfort provided by flexibility and superior impact resistance compared to neat Kevlar, thus making them a high-performance composite material and an essential component of body armor capable of meeting modern human protection requirements [53]. Shear-thickening fluids are generally produced by dispersing solid particles, such as silica [54] or calcium carbonate [55], into liquid media, typically ethylene glycol [56], polyethylene glycol, or similar carriers [57].

In recent years, a growing number of researchers and specialists in advanced materials have carried out extensive investigations, both experimental and numerical, with the aim of analyzing, in detail, the behavior and mechanical performance of Kevlar fabrics impregnated with shear-thickening fluids (STFs), highlighting their potential in ballistic protection applications. Xie et al. [58] showed, through rheological measurements and low-velocity impact tests performed at −30 °C, +20 °C, and +60 °C, that Kevlar fabrics impregnated with STF display markedly improved performance compared with neat Kevlar. At −30 °C, shear thickening occurs more easily, although the maximum viscosity is lower (209.448 Pa·s) and the STF absorbs up to 14.36 J, representing an 18.4-fold increase compared to the 0.78 J recorded at +60 °C. Under these low-temperature conditions, STF-treated Kevlar exhibited a 73% increase in peak force and a 75% increase in specific energy absorption relative to neat fabric. At +60 °C, although STF viscosity decreases substantially, the enhanced yarn mobility leads to a pronounced increase in frictional resistance during impact, resulting in a 300% rise in peak force and a 382% increase in specific energy absorption compared with neat Kevlar. These combined results demonstrate that the impact response of STF–Kevlar composites is governed not only by the intrinsic viscosity of the STF but also by temperature-driven changes in yarn–yarn friction. Therefore, their ballistic efficiency must be evaluated and optimized with respect to specific thermal conditions. In another recent study [59], the authors proposed a numerical fluid–structure interaction model for the STF–Kevlar system, based on the S-ALE algorithm and implemented in LS-DYNA, using the rheological curve of the STF as the constitutive model and comparing impact simulations with experimental data. The study demonstrated that STF viscosity evolves in three distinct stages (shear thinning, thickening, and recurrent thinning): the model accurately predicts projectile residual velocity and ballistic limits, STF-impregnated fabric exhibits reduced deformations and superior energy absorption compared to neat Kevlar—particularly at low impact velocities—and the energy is predominantly dissipated through the STF. These findings validate the methodology as an effective tool for designing protective materials in engineering applications without the exclusive need for physical testing.

In another study [60], picture-frame tests performed on neat Kevlar revealed a linear load–displacement response that remained unchanged with the loading rate. In contrast, Kevlar impregnated with STF exhibited a nonlinear curve characterized by locking loads and substantially higher energy absorption, especially within the shear-thickening regime. This improved behavior results from the rapid viscosity increase in the STF under shear, which restricts yarn mobility, enhances inter-yarn friction, and allows the fabric to withstand higher forces over larger displacements. Consequently, STF-treated Kevlar dissipated significantly more mechanical energy than the untreated fabric, confirming that shear-thickening-induced yarn confinement is a key mechanism responsible for the enhanced impact and deformation resistance of the composite. Enling Tang et al. [61] combined numerical simulation with experimental ballistic impact testing of a composite structure consisting of STF-impregnated Kevlar fabric applied to a glass fiber-reinforced plastic (GFRP) laminate. In their study, the simulated and experimental targets shared the same geometric configuration: a multilayer GFRP laminate modeled in TexGen as an orthogonal [0/90°] woven architecture, with each 1 mm of laminate thickness comprising six individual

glass–fiber layers embedded in an epoxy matrix, and a plain-weave Kevlar fabric modeled at the yarn scale as the representative unit cell. The STF layer was incorporated using a fluid–solid coupling approach to accurately reproduce its rheological behavior during impact. This explicit definition of laminate thickness, layer count, and yarn-level geometry ensured that the numerical model reproduced the scale and structural arrangement of the experimental composite panel. Xiaolian Wang et al. [62] impregnated Kevlar fabric with STF and obtained a composite with more than twice the load-bearing capacity and energy absorption compared to neat Kevlar. Adhesion tests demonstrated that aluminum surface treatments, particularly oxidation at 30 V for 20 min, improved bonding with STF–Kevlar, and analyses of 3/2 metal–composite laminates showed that incorporating STF increased energy absorption and reduced impact damage, achieving performance comparable to two layers of neat Kevlar but without back-face cracking.

Alexe F. et al. [63] investigated soft armor structures based on Kevlar® by integrating shear-thickening fluids (STFs), testing ten formulations, and demonstrating that only those containing PEG400 with 20–30% filler exhibited suitable behavior. They evaluated their performance under moderate impact, defined in the study as a drop-weight test based on ASTM D7136, in which a 1.004 kg blunt metallic projectile was released from a height of 1.5 m, corresponding to an impact energy of 14.77 J applied onto 10 × 10 × 1.5 cm STF specimens packed in polyethylene. Under these conditions, some formulations absorbed 45–55% of the kinetic energy, while formulation P10 reached 60%. Subsequently, they developed Kevlar–STF composite structures subjected to high-velocity impact tests, which showed that the spacing between Kevlar layers is critical for a ballistic response.

The optimal configuration was identified as formulation P4 (PEG400 + 30% Aerosil) placed between the first two of eleven Kevlar XP layers, being the only one capable of reducing the back-face signature and stopping the bullet. These findings were further confirmed through numerical simulations in Ansys AutoDyn.

Ultra-high-molecular-weight polyethylene (UHMWPE), commercially known as Dyneema®, has evolved from its early biomedical applications in the 1950s to the development of high-performance fibers and laminates in the late 1970s, and today represents an essential material in ballistic and blast protection systems due to its exceptionally high strength-to-weight ratio [64]. With a density of only ~0.93 g/cm^3 and a tensile strength typically ranging between 2.4 and 4.0 GPa, values that translate into a specific strength several times higher than that of steel and approximately 30–40% higher than that of UHMWPE aramid fibers is considered one of the highest-performing reinforcement fibers. This performance derives from its extremely long molecular chains and very high molecular weight (2–6 million g/mol), produced through ethylene polymerization followed by gel-spinning processing [65,66]. This process has been used to produce fibers for specialized applications, including personal armor, bulletproof vests, vehicle armor, cut-resistant gloves, mountaineering equipment, as well as suspension lines for parachutes and paragliders [67].

UHMWPE fibers exhibit a higher elongation at break and superior specific strength compared to aramid fibers, with failure strains of 3.8% versus 3.6% for aramid and tensile strengths of 3.6 GPa at a much lower density (970 kg/m^3 compared to 1440 kg/m^3). Their tenacity is also markedly higher (3.7 N/tex vs. 2.4 N/tex), which explains the enhanced energy absorption capability and why UHMWPE-based composites provide approximately 25% greater ballistic performance at equal areal densities [68,69].

Nabil Muzhaffar Effendi et al. [70] conducted a study developing two innovative sandwich-type bulletproof vest configurations based on UHMWPE, incorporating complementary materials (titanium Ti-6Al-4V and PVC) with the aim of achieving an optimal balance between ballistic protection, reduced weight, and comfort. The study highlighted the effectiveness of the UHMWPE + titanium + PVC layered design in ballistic protection,

resulting in complete bullet stoppage without penetration, with performance confirmed both experimentally and through FEM simulations. Yongji Gao et al. [71] carried out ballistics tests (12.7 mm AP) on sandwich plates consisting of SiC as the strike face, a Ti-6Al-4V interlayer, and a UHMWPE backing. Their results showed that SiC/UHMWPE and Ti-6Al-4V/UHMWPE targets exhibited superior penetration resistance compared to the triple-layer configuration (SiC/Ti-6Al-4V/UHMWPE) at equal areal density, since the titanium interlayer reduced the effective thickness of both SiC and UHMWPE. This finding underscores the importance of layer thickness in ballistic protection. Nayan Pundhir et al. [72] compared the performance of UHMWPE composite laminates with those of traditional Kevlar/epoxy composites, focusing on the influence of thickness, layered structure, and impact angle on ballistic protection, thereby demonstrating the potential of UHMWPE as an optimal material for lightweight and energy-efficient armor.

2.4. Composite Materials

The development of innovative composite materials, obtained by exploiting existing materials, represents a significant challenge for most materials engineers. Nevertheless, extensive research efforts are being carried out, aimed at producing materials with enhanced mechanical, electrical, and thermal properties [73].

Composites combine different materials to exploit complementary properties. In ballistic protection, they often include combinations of metals, polymers, and ceramics, while hybrid versions with varied layers provide an optimized response to different types of impacts [74,75]. Layered composites, produced by integrating ceramic plates with polymeric backings, simultaneously ensure hardness and flexibility, thereby optimizing ballistic resistance. Such advanced structures represent a paradigm shift in the design of protective materials, as the combination of multiple components leads to enhanced properties [76]. These composites, commonly manufactured from fibers such as aramid or ultra-high-molecular-weight polyethylene embedded in a matrix, stand out for their exceptional strength and flexibility. Their layered architecture further enhances ballistic performance while offering an outstanding strength-to-weight ratio, enabling them to provide protection levels equivalent to or superior to traditional metals, but at a significantly reduced weight [77].

Ballistic composites can be designed to meet specific performance requirements while maintaining high impact resistance, thereby becoming multifunctional materials [78,79].

Fiber-reinforced polymer matrix composites are currently considered among the most promising solutions for protection against high-velocity impacts due to their superior performance. They combine high mechanical strength with low weight and an enhanced ability to absorb and dissipate energy, achieved through mechanisms such as fiber breakage and matrix cracking [7,80,81]. Fiber-reinforced polymer (FRP) matrices are recognized as high-performance armor materials, offering an excellent strength-to-weight ratio as well as efficient impact energy absorption capacity.

In a recent study, Evangelos et al. [82] designed, manufactured, and tested three advanced laminated composite armor systems according to STANAG Level 4 standards. The first system incorporated a backplate made of an AA2024 metal matrix composite (MMC) reinforced with MWCNTs (multi-walled carbon nanotubes), while the other two variants used conventional backplates. All composite plates were mechanically clamped onto a 7 mm steel chassis, which served as both structural support and ballistic backing during the STANAG tests. Comparative ballistic evaluation showed that all plates successfully met the required performance criteria; however, the MMC–CNT configuration demonstrated superior mechanical and ballistic behavior, reduced weight, and enhanced kinetic energy absorption through plastic deformation and post-impact fracture mecha-

nisms. It also exhibited improved bending recovery characteristics and was identified as a promising alternative to monolithic RHA steel armor. Furthermore, the design and testing methodology presented by the authors represents the first holistic Greek approach for the development of passive composite armors intended for military vehicle protection. A concise classification of the main material classes used in ballistic protection, together with their representative materials, key characteristic properties, and corresponding references, is presented in Table 1, providing an overview of the mechanical, structural, and functional attributes that underpin their performance in armor systems.

Table 1. Key materials used in ballistic protection.

Class of Materials	Material	Characteristic Properties	Typical Range of Key Physical Properties	Ref.
Metals	Armox 500T	High-strength ballistic steel; Good combination of strength and toughness; Used for ballistic protection applications.	Hardness: 480–540 HB; Yield strength: 1200–1600 MPa; Density: 7.8 g/cm^3	[20–24]
	Hardox 450	High hardness and abrasion resistance; Superior ductility and toughness; Suitable for ballistic barriers and hybrid armor systems.	Hardness: ~450 HB; Yield strength: 1200 MPa; Density: 7.85 g/cm^3	[21–25]
	PROTAC 500	High-strength steel used in ballistic applications; Recognized for strength and toughness.	Hardness: ~480 HB; Yield strength: 1300–1500 MPa	[20–24]
Ceramics	Al_2O_3 (Alumina)	High hardness, stiffness, thermal resistance, environmental stability; Low cost and good manufacturability.	Hardness: 14–20 GPa; Density: 3.8–3.95 g/cm^3; Elastic modulus: 300–400 GPa	[27–32]
	SiC (Silicon Carbide)	Lower density than alumina; Higher hardness and fracture strength than alumina; Ballistic performance close to B_4C but with much lower cost; Intermediate balance between cost, toughness, manufacturability, and ballistic efficiency.	Hardness: 22–28 GPa; Density: 3.15–3.25 g/cm^3; Elastic modulus: 380–420 GPa	[30,31,33, 36]
	B_4C (Boron Carbide)	Extremely low density, very high hardness, highest ballistic efficiency; Limitation: stress-induced amorphization decreases shear strength and ballistic resistance; Amorphization controlled by composition and microstructure.	Hardness: 30–38 GPa; Density: 2.48–2.52 g/cm^3; Elastic modulus: 450–470 GPa	[30–35]
Polymers	Kevlar	Low density: ~1.44 g/cm^3; High tensile strength and high elastic modulus; High strength-to-weight ratio, approx. five times stronger than steel on equal weight basis; Large failure strain and efficient in-plane energy distribution (fibrillation + fiber stretching); Excellent chemical stability, low thermal expansion, good dimensional stability, high rigidity. High flexibility, enabling comfort and mobility in soft armor; Exceptional ballistic performance, significantly enhanced when impregnated with STF.	Density: 1.44 g/cm^3; Tensile strength: 2.8–3.6 GPa; Modulus: 70–130 GPa; Failure strain: 2.5–4%	[41–52]
	UHMWPE	Very low density: ~0.93 g/cm^3/970 kg/m^3; Extremely high strength-to-weight ratio; Tensile strength: 2.4–4.0 GPa; Specific strength 30–40% higher than aramid fibers; Very high molecular weight: 2–6 million g/mol; Failure strain: 3.8% (vs. aramid 3.6%); Tenacity: 3.7 N/tex (vs. aramid 2.4 N/tex); ≈25% higher ballistic performance than aramid at equal areal density; Excellent energy absorption capability.	Density: 0.93–0.97 g/cm^3; Tensile strength: 2.4–4.0 GPa; Modulus: 80–120 GPa; Failure strain: 3.5–4%	[64–72]
Composite	AA2024 metal matrix composite reinforced with MWCNTs (MMC–CNT)	Enhanced mechanical behavior compared to conventional backplates; Superior ballistic performance under STANAG Level 4 testing; Reduced weight relative to standard metallic backplates; Higher kinetic energy absorption.	Density: 2.75–2.80 g/cm^3; Tensile strength (reinforced): 500–600 MPa; Modulus: 70–80 GPa	[82]

Despite the remarkable progress made in the development of metals, ceramics, polymeric fibers, and composite systems for ballistic protection, several scientific and technological challenges remain open and continue to define the research landscape. One major challenge is achieving an optimal balance between weight reduction and high ballistic efficiency, particularly for next-generation ceramic and UHMWPE-based systems, where improvements in performance often come with increased cost or processing complexity. For metallic and ceramic armors, brittleness, multi-hit capability, and long-term durability under harsh environmental conditions remain critical limitations that require new solutions in alloy design, microstructural engineering, and damage-tolerant architectures. For polymeric fibers such as aramids and UHMWPE, research opportunities include enhancing inter-yarn friction, improving thermal stability, and developing multifunctional surfaces ca-

pable of resisting combined mechanical, thermal, and chemical threats. Composite armors also face challenges related to interfacial adhesion, energy dissipation mechanisms, and the optimization of hybrid-layered architectures. Furthermore, understanding the strain-rate-dependent behavior of advanced materials and validating their response through multiscale modeling remains essential for designing lighter and more efficient protective systems. Overall, these challenges highlight the need for continued innovation in materials engineering, interfacial modification, and structure–property optimization to enable the next generation of high-performance ballistic protection solutions.

3. Coatings for Ballistic Enhancement

As weapons evolve, ballistic armor must keep pace with increasingly demanding requirements, and one research direction focuses on the use of coatings and novel materials to enhance personal protection [83,84]. The aim is to provide soldiers and law-enforcement personnel with a higher level of protection without compromising mobility by implementing thin coating layers that reduce weight and increase flexibility. This approach paves the way for new techniques capable of modifying the properties of conventional materials and generating more adaptable defense systems [84].

These functional coatings are specialized finishes applied to textiles to impart additional properties that enhance performance and functionality, while also contributing to increased comfort, safety, and durability [85].

To reduce weight and enhance wearer mobility, researchers have developed soft vests based on textiles. However, although this solution partially decreases the mass of body armor, ballistic performance is typically ensured by adding multiple layers, which inevitably leads to an increase in weight [86]. With the advancement of nanotechnology, researchers have begun integrating nanoparticles into the structure of soft body armor, applied as coatings on the surface of textiles to impart superior ballistic properties. This approach allows for a reduction in the number of required layers and, consequently, in the overall weight of bulletproof vests, while maintaining the desired level of protection [87].

Nanotechnology, defined as the manipulation of materials at the nanometer scale (with at least one dimension <100 nm) [88], has gained significant attention in the field of ballistic protection due to the high surface-to-volume ratio and unique structural architecture of nanomaterials, which provide them with very high strength and modulus as well as remarkable energy absorption capacity [89].

3.1. Coating Methods Used in Ballistic Protection

Over time, techniques for coating fiber surfaces with various materials have evolved significantly. Between 1990 and 2010, representative methods included sol–gel processing, physical vapor deposition (PVD), chemical vapor deposition (CVD), thermal spraying, and electroplating [90]. In addition to these, advanced approaches such as nanoparticle deposition, electrophoretic deposition (EPD), atmospheric plasma spraying, spray coating, RF plasma-assisted CVD (RF-PECVD), and flame synthesis have been employed to enhance the flexural, tensile, and thermal properties of fibers and fabrics [91–95].

In general, the hydrophilic nature of natural fibers favors interfacial adhesion but causes swelling when exposed to environmental conditions, which limits their use in bulletproof armor [96]. To overcome this drawback, coatings with polymers, metal oxides, or nanoparticles can render the surface hydrophobic and increase ballistic impact resistance, while potential coating techniques for anti-impact textiles are illustrated in Figure 2 below.

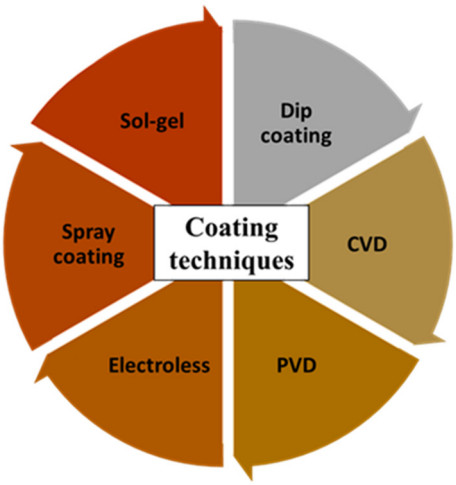


Figure 2. Coating techniques used in ballistic protection.

3.1.1. Sol–Gel Deposition Method

The sol–gel process is a wet-chemical technique in which synthesis begins with obtaining a homogeneous solution by dissolving the precursor in a solvent medium (water or an organic solvent)—a critical step regardless of whether the raw material is an inorganic salt or a metal alkoxide [97,98]. The sol–gel method involves four main stages (as shown in Figure 3)—(1) hydrolysis of the precursors, (2) condensation and polymerization of monomers into chains and particles, (3) particle growth, and (4) agglomeration of polymeric structures—and the formation of a continuous network throughout the liquid medium, ultimately leading to thickening and gel formation [99,100].

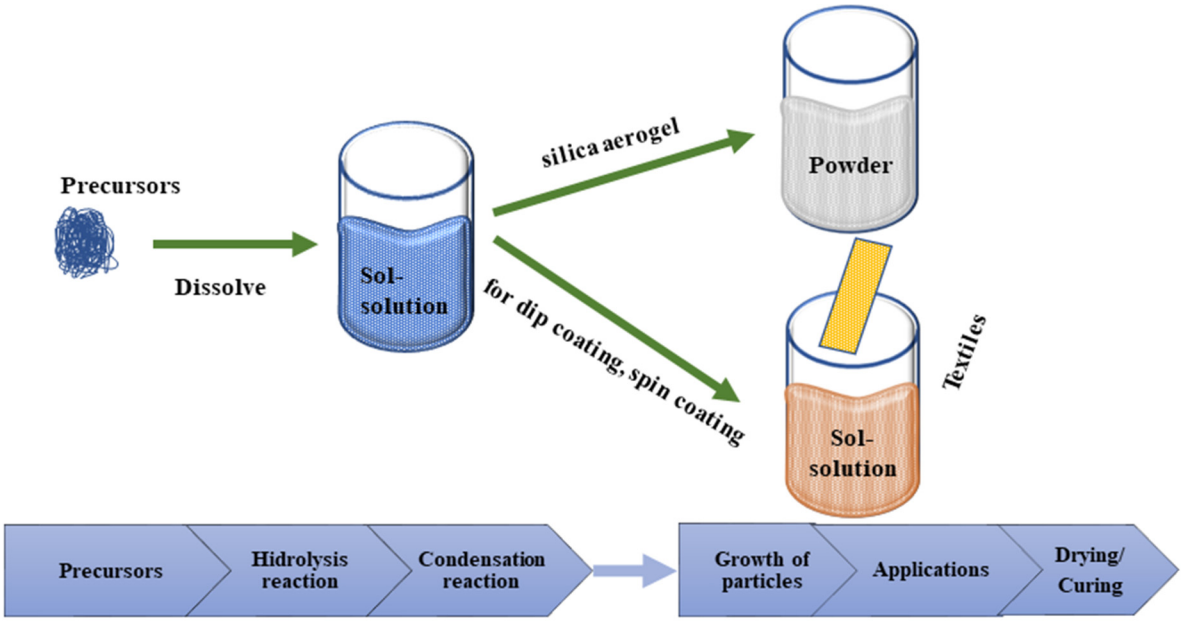


Figure 3. Schematic representation of the sol–gel process.

The sol–gel technology is a common surface coating method capable of depositing layers onto fibers and thereby modifying their surface morphology. This method starts from colloidal suspensions obtained through the hydrolysis of suitable precursors, mainly organometallic compounds, catalyzed by either acids or bases [101,102]. Through the polycondensation of the hydrolysis products, an oxide skeleton gradually forms in the solution (the gel). In the coating process, the sol is applied onto the fiber or fabric, followed by drying at an elevated temperature to remove the liquid phase and generate a thin porous

layer on the fiber surface, and then by an additional thermal treatment that completes the polycondensation and transforms the layer into a crosslinked gel physically and, in some cases, chemically bonded to the substrate [103,104].

A study by Chu et al. [105] coated Twaron aramid fibers using the sol–gel method with TiO_2/ZnO hydrosols of either submicrometric or nanometric particle size in order to modify surface morphology and enhance inter-yarn friction. SEM and spectroscopic analyses confirmed the deposition of TiO_2/ZnO layers, with the submicrometric hydrosol forming a rough, sheet-like ceramic coating that created larger surface asperities, while the nanometric hydrosol produced a smoother and more uniform film. The submicrometric treatment led to a substantial increase in inter-yarn friction, approximately 54% relative to untreated fibers, whereas the nanometric coating achieved only about 10% improvement. These findings indicate that the sol–gel route enhances inter-yarn friction primarily through mechanical interlocking induced by surface roughening, with minimal impact on mass or tensile strength, making it a promising strategy for lightweight ballistic armor systems. Beyond these individual studies, recent advances further confirm the relevance of the sol–gel process as a frontier technique in ballistic textile engineering. Several reports highlight that sol–gel coatings allow precise control over layer thickness, porosity, and surface roughness parameters directly linked to frictional behavior and energy dissipation mechanisms during impact. The method has been successfully applied to produce hybrid ceramic–polymeric networks, multifunctional oxide coatings, and nanostructured films capable of improving mechanical anchoring between yarns while adding negligible mass to the fabric. Moreover, the sol–gel route is compatible with large-scale textile finishing lines, offering an industrially viable alternative to more complex techniques such as hydrothermal nanowire growth or vacuum filtration. Sol–gel-based coatings consistently yield measurable improvements in inter-yarn friction, energy absorption, and ballistic response, demonstrating both scientific maturity and strong translational potential within next-generation lightweight armor systems. In a subsequent study, Yanyan Chu and colleagues [106] extended the research to Twaron fabrics, combining experimental work with numerical modeling to show how the increase in inter-yarn friction achieved through the sol–gel method influences ballistic performance.

3.1.2. Dip-Coating Deposition Method

The dip-coating process involves immersing the substrate into a liquid precursor solution, which may be either water-based or formulated with organic solvents, depending on the nature and solubility of the coating materials [107–109]. After immersion, a liquid film adheres to the surface during withdrawal, levels under gravity and viscous forces, and subsequently dries into a solid layer. Dip coating can be applied in both continuous and batch modes and is widely used for depositing conductive polymers, carbon-based structures, inorganic (nano)particles, or hybrid systems on textile substrates [110–113]. The main stages of the process from immersion and film formation to solvent evaporation and final layer consolidation are schematically illustrated in Figure 4.

Recent developments in dip coating demonstrate that this method remains a cornerstone in the functionalization of ballistic textiles due to its scalability, uniformity, and compatibility with a wide range of coating chemistries. Studies have shown that dip coating enables the controlled deposition of ceramic nanoparticles, polymeric binders, sol–gel-derived oxides, and shear-thickening fluids, each contributing to enhanced friction, stiffness, and impact energy dissipation. For instance, nanosilica-based STF systems applied by dip–pad–dry sequences have been proven to increase specific energy absorption and reduce yarn pull-out, while metal-oxide hydrosols deposited via dip coating significantly improve inter-yarn friction with negligible added weight. Furthermore, dip coating

allows multilayer deposition with tunable thickness, an important parameter for balancing flexibility and ballistic performance. Coatings applied through dip coating consistently yield quantifiable improvements in tensile response, inter-yarn friction, and ballistic resistance, emphasizing the method's versatility and industrial feasibility for next-generation lightweight armor solutions.

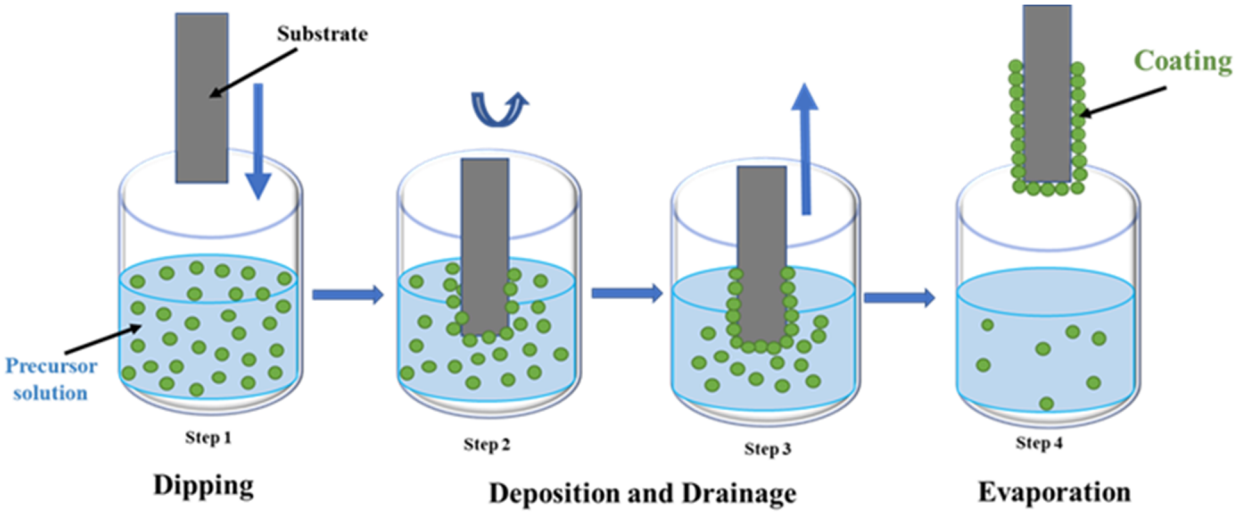


Figure 4. Schematic representation of the dip-coating process.

3.1.3. Physical Vapor Deposition Process

The PVD technique is a thin-film deposition process in which the layer grows on the substrate atom by atom. The process involves atomizing or vaporizing a material from a solid source (target), resulting in films with thicknesses ranging from a few atomic layers to several microns, as can be seen in Figure 5. This type of deposition induces modifications both at the surface level and within the transition zone between the substrate and the deposited material, with the resulting properties also depending on the characteristics of the substrate. Atomic deposition can be carried out in vacuum, gaseous, plasma, or electrolytic environments, with the use of vacuum in the deposition chamber significantly reducing gaseous contamination and ensuring high-quality films [114,115].

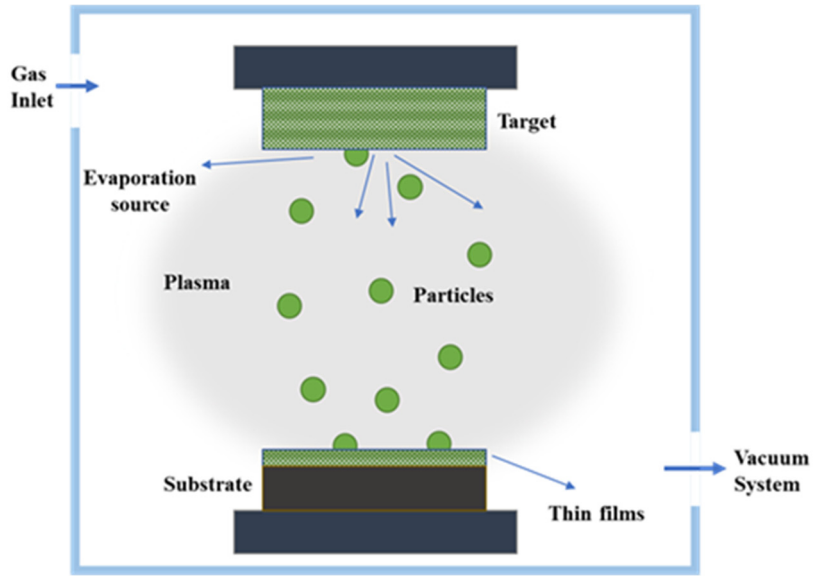


Figure 5. Schematic diagram of the physical vapor deposition (PVD) process.

PVD shows high potential for application across a wide range of fields, including the aerospace, automotive, biomedical, and defense industries [116].

In recent years, PVD has gained increasing attention in the ballistic materials community due to its ability to produce ultra-dense, conformal, and adherent coatings that significantly modify surface hardness, abrasion resistance, and interfacial bonding properties directly linked to ballistic performance. Cutting-edge studies report the successful deposition of ceramic layers such as TiC, TiN, and Al_2O_3, or multilayer nano-architectures, which enhance fiber stiffness and improve resistance to cutting, tearing, or high-velocity particle impacts. Additionally, PVD enables nanoscale engineering of the coating–substrate interface, promoting better load transfer and reducing premature fiber failure under dynamic loading. While its use on woven fabrics remains experimentally challenging due to substrate flexibility, advances in plasma-assisted PVD and low-temperature sputtering have opened new pathways for depositing protective ceramic and metal-oxide films on aramid and UHMWPE fibers. Thin PVD-derived coatings can provide measurable improvements in mechanical reinforcement and impact resistance, positioning PVD as a promising though still emerging approach for high-performance ballistic textiles where superior surface hardness and energy dissipation are required.

3.1.4. Chemical Vapor Deposition Process

Chemical vapor deposition (CVD) is a widely used technology for producing thin films and coatings, playing an essential role in industries such as semiconductors, optics, and nuclear fuels. The process involves chemical reactions of volatile precursor gases at the substrate surface, resulting in the formation of a solid deposited layer [117].

The general reaction sequence of the CVD process can be described in five main steps: (1) introduction of reactive gases into the reactor by forced flow, followed by (2) their diffusion through the boundary layer situated between the bulk gas flow and the stagnant layer at the substrate surface. Subsequently, (3) the gases reach the substrate surface, where (4) deposition reactions occur, and finally, (5) the gaseous by-products diffuse back through the boundary layer and are exhausted. The overall rate of the process is controlled by the slowest step, which is typically either the surface chemical reaction (step 4) or mass transport through the boundary layer (step 2). Parameters such as temperature and pressure directly influence this rate-limiting step, having a significant impact on the microstructure of the deposited layer [118,119].

However, CVD equipment is expensive to operate and maintain, precursors are inherently reactive, often flammable, and sometimes highly toxic, and many CVD processes are truly versatile only above ~600 °C, excluding numerous substrates. Some of these limitations, however, can be overcome by employing lower-temperature techniques such as plasma-enhanced CVD (PE-CVD) and laser-assisted CVD (LA-CVD) [120–123].

In the scientific literature, numerous studies report the use of PACVD for surface modification of ballistic textile materials, particularly para-aramid and UHMWPE fibers, demonstrating significant improvements in abrasion resistance, thermal stability, and durability of ballistic performance [124–127].

Recent advancements in CVD technologies have expanded their applicability to high-performance ballistic textiles by enabling the deposition of highly uniform, strongly adherent, and chemically robust protective layers at the nanometer scale. Plasma-assisted CVD (PACVD) has been particularly effective for depositing diamond-like carbon (DLC), silicon-based coatings, and nitrides on para-aramid and UHMWPE fibers, significantly enhancing interfacial adhesion, resistance to fibrillation, and thermo-oxidative stability factors that directly influence ballistic durability under repeated impacts. Under controlled plasma conditions, PACVD coatings can increase fiber–fiber friction, reduce yarn slip-

page, and delay the onset of fiber rupture during high-velocity loading. Additionally, low-temperature CVD variants mitigate thermal degradation of polymeric substrates, allowing for conformal coating on delicate ballistic fabrics. These engineering achievements demonstrate that CVD, although more capital-intensive than dip-coating or sol–gel routes, offers unique advantages in tailoring microstructural features and surface chemistry at the molecular level. CVD-derived coatings contribute to measurable improvements in abrasion resistance, thermal endurance, and energy dissipation mechanisms, positioning this method as a promising solution for long-term durability and next-generation ballistic protection systems.

3.1.5. Spray Coatings

Spray coating is a versatile deposition technique in which a nozzle atomizes the coating solution into fine droplets that are transported toward the substrate. Although spraying onto a preheated substrate is frequently employed to enhance solvent evaporation in certain applications, it is not a general requirement for the technique. Spray coating can be performed at room or elevated temperature, depending on the coating formulation and desired microstructure. The process consists of four main stages: droplet atomization, transport, coalescence on the substrate, and drying or post-deposition curing. While low-surface-tension solvents may facilitate wetting, successful spray deposition can also be achieved with waterborne formulations. More generally, good wetting requires the surface tension of the liquid coating to be compatible with—or lower than—the surface free energy of the substrate; additionally, pre-treatments can be applied to improve adhesion and layer uniformity [128–130].

Recent research highlights spray coating as a highly versatile and scalable technique for functionalizing ballistic textiles with nanomaterials, polymeric binders, or hybrid ceramic–polymeric suspensions. Its capability to deposit thin, homogeneous layers over large and irregular surfaces makes it particularly suitable for aramid and UHMWPE fabrics. Emerging studies report successful applications of spray-coated silica-based STFs, graphene nanoplatelets, metal-oxide sols, and conductive nanomaterials, leading to measurable improvements in frictional behavior, tensile reinforcement, and localized energy dissipation during impact. Unlike immersion-based methods, spray coating enables precise control over deposition thickness, droplet size, and material distribution, allowing the fabrication of gradient or multilayer structures tailored for ballistic performance. Moreover, the low-temperature nature of the process prevents thermal degradation of polymeric fibers and maintains the mechanical integrity of the substrate. Spray-coated systems have demonstrated enhanced inter-yarn friction, improved energy absorption, and superior impact mitigation, positioning spray deposition as an efficient and industrially attractive route for integrating advanced nanostructured coatings into next-generation lightweight ballistic fabrics.

3.2. Coatings for Enhanced Ballistic Performance

In ballistic applications, energy absorption efficiency is improved by optimizing interfacial properties, and the addition of nanoparticles such as nanosilica [131], graphene [132], carbon nanotubes (CNTs) [133], zinc oxide (ZnO) [134], or nanoclay [135] onto high-performance fibers enhances impact resistance. The final performance depends on the type of fibers and matrix, the proportion and dispersion of nanoparticles, as well as interfacial interactions.

3.2.1. Nanosilica Coatings

Silica has attracted significant interest in materials science as a reinforcing nanofiller due to its combination of remarkable properties, including a high elastic modulus (approximately 70 GPa), large specific surface area (50–380 m^2/g), excellent thermal stability (up

to 1200 °C), low density (1.8 g/cm^3), a low coefficient of thermal expansion, and good abrasion resistance. Chemically, silica consists of silicon dioxide (SiO_2) and can occur in both crystalline and amorphous forms [136].

Khodadadi et al. [47] successfully demonstrated that impregnating Kevlar with an STF based on silica nanoparticles (in PEG), at an optimal concentration of around 35% nanosilica, can significantly enhance the ballistic performance of the fabric by increasing the energy absorbed during impact and the inter-fiber friction. Their impact tests showed that increasing the nanosilica content from 15% to 35% led to a pronounced rise in energy absorption, while further increasing it to 45% produced only marginal improvement, confirming that 35% provides the highest specific energy absorption per unit mass. This indicates that ballistic enhancement is achieved without a meaningful increase in areal density, thereby offering a demonstrably favorable weight efficiency for STF/Kevlar composites. In another study [137], Feng and colleagues investigated how the size and concentration of two distinct types of silica particles, fumed silica at a 20 wt% fraction and submicron silica at a 65 wt% fraction, influence the performance of aramid fabrics impregnated with shear-thickening fluids. Through quasi-static stabbing tests, single-fiber tensile tests, and pull-out tests, they demonstrated that the use of silica particles with markedly different particle sizes and weight proportions significantly alters puncture resistance and the underlying fiber–fiber interaction mechanisms. Obradovic et al. [138] showed that the addition of 30 wt% silane-modified nanosilica (AMEO silane) into a hybrid layer with aramid (Kevlar) significantly increases ballistic shock resistance. Compared to composites without nanosilica, the treated ones exhibited reduced penetration depth in live-fire weapon tests. Çolpankan Güneş and colleagues [139] demonstrated that impregnating aramid fabrics with nanosilica-based shear-thickening fluids leads to a pronounced shear-thickening rheological behavior, a significant increase in quasi-static and dynamic puncture resistance, and an improvement in ballistic limits (V_{50}). All of these enhancements were achieved without compromising the flexibility of the fabric, confirming nanosilica's role as a key element in improving the performance of protective materials.

3.2.2. Coatings Based on Graphene

Graphene, regarded as the most representative two-dimensional (2D) material, consists of sp^2-hybridized carbon atoms [140]. It is an atomic-thick membrane composed of a single layer of carbon atoms arranged in a two-dimensional hexagonal lattice, representing the fundamental building block of graphite, and is recognized as an exceptional material due to its extraordinarily high intrinsic strength, stiffness, and remarkable thermal, electrical, and mechanical properties [141,142].

The properties of graphene are mainly influenced by its average lateral size, the number of layers, and the carbon-to-oxygen ratio. A key aspect is the isolation of individual layers, since only in this state can the unique properties of graphene and its composites be achieved; otherwise, the sheets tend to aggregate, forming graphite-like structures [143,144]. Owing to the combination of its extremely high Young's modulus (~1 TPa), fracture strength (~130 GPa), and low density (≈2200 kg/m^3), graphene is considered an ideal material for ballistic protection applications [145,146]. A major focus of current research is the use of graphene as a protective membrane against ballistic impacts, with the literature suggesting its application in bulletproof vests for stopping high-velocity projectiles [5,147].

Although graphene sheets have previously been employed in body armor to reduce blunt trauma and dissipate the projectile's kinetic energy away from the impact zone, the high cost of producing graphene platelets has, with the advancement of nanotechnology, shifted research toward the use of graphene nanoparticles and nanoplatelets applied onto the surface of high-performance fabrics. This approach has led to measurable improve-

ments in the mechanical properties of the resulting nanocomposites, with several studies reporting increases of 20–50% in tensile strength, 10–40% in Young's modulus, and significant enhancements in toughness due to mechanisms such as improved load transfer at the graphene–matrix interface, crack deflection, and reduced fiber pull-out [74]. Graphene oxide (GO) is a derivative of graphene, characterized by the presence of oxygen-containing functional groups such as hydroxyl, epoxy, and carboxyl groups attached to the graphene layer surface. It is a two-dimensional material consisting of a single atomic layer arranged in a hexagonal lattice. Due to these functional groups, graphene oxide exhibits high hydrophilicity and easily disperses in many polar solvents, including water and organic solutions. Moreover, its structure allows easy functionalization through the attachment of additional molecules or nanoparticles to the surface. In general, graphene oxide is synthesized from graphite, a crystalline form of carbon, using strong oxidizing agents such as potassium permanganate or sodium nitrate [148–151].

Owing to its remarkable mechanical properties, graphene has been extensively studied for impact protection applications. Anderson Oliveira da Silva et al. [152] reported a significant improvement in the ballistic performance of aramid fabrics coated with graphene oxide (GO), demonstrating an up to 50% increase in absorbed energy compared to untreated fabric, attributed to the better adhesion of GO to fibers and increased inter-fiber friction. Kukle S. and colleagues [153] developed an original method of applying a graphene layer to para-aramid fibers, ensuring strong adhesion to the fiber surface while avoiding costly extraction and redispersion processes. This method was also found applicable for modifying polyamide fibers. By integrating graphene-modified aramid layers into hybrid ballistic packages, the authors demonstrated quantifiable improvements: in several configurations, replacing five UD XP layers with only three graphene-modified KM2-600 layers reduced the total layer count and areal density by up to 8%, while decreasing the BFS by ~10%. In hybrid systems based on Kevlar XP™ K520, the inclusion of graphene-modified layers led to a substantial reduction in penetration depth, up to 44%, without significantly increasing the areal density. These results confirm that graphene functionalization enhances structural stability, restricts fiber slippage, and improves energy dissipation, thereby markedly increasing the ballistic performance of the soft armor package. Costa et al. [154] coated natural fibers with graphene oxide and incorporated them into epoxy composites for layered armor systems. They achieved significantly improved adhesion to the matrix, enhanced thermal resistance, and ballistic performance comparable to that of Kevlar laminates of the same thickness, successfully stopping 7.62 mm projectiles without requiring an additional ductile metallic layer.

The study [140] demonstrates that coating silicon carbide with graphene layers significantly enhances ballistic performance. Bilayer graphene provides the best indentation resistance, while at five layers, the ballistic limit velocity increases by 69.4% and the specific penetration energy by 43.3% compared to uncoated silicon carbide. The graphene layer rapidly dissipates impact energy through stress wave propagation and resists projectile penetration via interlayer transitions and bond breakage. The influence of temperature is minimal, and secondary impacts can further improve performance through sp^3 bond formation and residual deformations. These results confirm the potential of graphene/silicon carbide laminates for the development of lightweight, high-strength armor.

Similarly, Mohammad Reza et al. [155] showed, through ReaxFF simulations (Reactive Force Field, a molecular dynamics force field capable of modeling bond formation and breakage), that graphene oxide (GO) layers applied to silicon carbide improve penetration resistance and alter nanoindentation and impact behavior. Samples with high oxidation (50%) increased adhesion to the substrate and inhibited crack initiation, promoting a brittle-to-ductile transition and localizing fracture in the impacted zone. Overall, GO layers can

be optimized according to the degree of oxidation to serve as protective coatings and reinforcements for ceramics. The author's further plan to test multilayer GO samples at elevated temperatures.

Lin et al. [156] reported the fabrication of laser-induced graphene (LIG) on polyamide substrates and its integration into basalt fiber-reinforced epoxy composites (LIG/BF/EP). These laminates exhibited good interfacial toughness, superior energy absorption capacity under ballistic loading, and enhanced EMI shielding efficiency (up to ~50 dB with three layers of LIG). Another study [157] demonstrated that integrating LIG into aramid fiber-reinforced composites not only improves mechanical and ballistic performance but also enables in situ detection of impact and delamination by monitoring changes in electrical resistance, which directly correlate with projectile velocity and damage severity. Thus, while the first study highlighted the role of LIG in enhancing energy absorption capacity and EMI shielding in basalt fiber composites, the second emphasizes the multifunctionality of LIG-treated aramid composites, providing both improved ballistic protection and self-monitoring damage detection capability.

3.2.3. Coatings with Carbon Nanotubes

Carbon nanotubes (CNTs) are hollow cylindrical structures derived from two-dimensional graphene sheets, with their surfaces composed of pentagonal and hexagonal rings of carbon atoms. They are considered one-dimensional nanomaterials due to their nanometer-scale diameter and lengths that can reach up to ~1 mm, which gives them extremely high aspect ratios as well as remarkable properties, such as outstanding mechanical strength and high thermal conductivity. These characteristics are attributed to the strong bonding between carbon atoms and the propagation of their vibrational modes. Being among the strongest known nanomaterials, CNTs exhibit a tensile strength of approximately 200 GPa, an elastic modulus exceeding 1 TPa, and relatively low density, making them highly advantageous for the development of high-performance nanocomposites for advanced applications [89].

Carbon nanotubes are classified into two major types: single-walled carbon nanotubes (SWCNTs), obtained by rolling a single graphene sheet into a cylinder, and multi-walled carbon nanotubes (MWCNTs), consisting of multiple concentric graphene cylinders held together by Van der Waals forces. Both the synthesis method and the intrinsic properties of these structures decisively determine their areas of application, ranging from materials science and electronics to nanotechnology and biotechnology [158].

The integration of carbon nanotubes into composites, particularly those based on aramid fibers such as Kevlar, has proven promising for improving soft armor, as it enhances interfacial adhesion and interactive properties and increases fracture toughness, energy absorption, tensile strength, and interlaminar shear resistance. Furthermore, through strategies such as functionalization, hybrid composites, or the use of standalone CNT sheets, uniform dispersion and improved mechanical resistance can be achieved. At the same time, the inherent conductivity of CNTs opens new opportunities for the development of smart armors and wearable electronic textiles capable of providing enhanced protection, force detection, and human motion monitoring [159].

Numerous studies have investigated the improvement in the ballistic performance of materials through the application of carbon nanotube (CNT)-based coatings [133,160–167]. Saisai Cao et al. [168] demonstrated that optimizing the volume fraction of particles in STFs and adding 1 wt% CNTs significantly enhances the ballistic performance of Kevlar composites. Experimental tests and numerical simulations confirmed that these modifications increase inter-fiber friction, homogenize stress distribution, and improve ballistic limit velocity as well as dissipated energy. Nakonieczna Dąbrowska et al. [169] formu-

lated silica/PPG-based STFs doped with carbon nanofillers (MWCNTs, rGO, GO, carbon black), performed microstructural and rheological characterizations, and tested them under impact on impregnated textiles. MWCNTs proved the most effective, lowering the shear-thickening threshold, increasing maximum viscosity (~5× compared to pure STF), improving long-term stability, and raising force absorption up to ~78% (~+12% over CNT-free STF). In another study [170], a layer of multi-walled carbon nanotubes (MWCNTs) was deposited on Kevlar yarns and fabrics to increase inter-yarn friction, with performance evaluated through tensile, friction, yarn pull-out, and low-velocity impact tests. Results showed an approximately 50% increase in the ballistic limit with negligible mass addition, correlated with significantly higher friction coefficients and pull-out forces, attributed to the entanglement effect of CNTs and increased surface roughness.

Mei Liu et al. [171] developed a wearable electronic textile material based on CNT/STF/Kevlar, combining superior ballistic protection performance with sensing functionalities. Yarn pull-out and stabbing resistance tests demonstrated a significant increase in impact resistance, with the composite reaching a maximum resisting force nearly twice that of neat Kevlar. In dynamic evaluations, the single-layer sample recorded a value of 1232 N compared to 746 N for Kevlar, highlighting its enhanced energy absorption capacity. Moreover, due to the electrical conductivity of CNTs, the composite exhibited body-motion monitoring capabilities, making it a promising candidate for wearable electronic textiles characterized by flexibility, sensitivity, and advanced protection.

Dhiwar et al. [172] produced composites based on Kevlar and epoxy resin, as well as Kevlar/epoxy resin reinforced with 0.5 wt% carbon nanotubes. Mechanical testing showed that the addition of CNTs improved tensile strength by 25%, an effect attributed to epoxy toughening and crack deflection enabled by the presence of highly resilient CNTs in the modified Kevlar/epoxy composites.

Lu and colleagues [173] developed a high-performance protective composite by combining shear-thickening fluids (STFs) and carbon nanotubes (CNTs) with Kevlar fabrics, employing an innovative preparation method using a 1% polyvinyl alcohol solution as a binder to achieve more effective integration between CNTs and Kevlar fibers. The resulting composite exhibited a 46.4% increase in tensile strength, a 23% reduction in residual velocity, and a 240.2% improvement in absorbed energy compared to neat Kevlar.

3.2.4. Zinc Oxide Nanowire (ZnO NWs) Coatings

In recent years, the functionalization of fabrics with ZnO nanoparticles has emerged as a promising strategy for improving low-velocity impact resistance. By grafting ZnO onto the fiber surface, inter-yarn friction is increased, thereby optimizing the anti-impact behavior of fabrics under stabbing/penetration conditions [134,174,175].

Yanyan Chu et al. [176] grew ZnO nanowires on satin-woven para-aramid fabrics and showed that they significantly improve tensile strength and interfilament friction, reduce panel weight and back-face signature (BFS) depth, while maintaining flexibility and comfort, though they do not provide advantages in direct ballistic energy absorption. Gowthaman et al. [177] coated plain- and twill-woven Kevlar fabrics with ZnO nanowires using a low-temperature hydrothermal growth method, demonstrating that this modification leads to uniform fiber coverage, increased deformation energy, higher inter-yarn friction, and improved ballistic energy absorption, all achieved with only a marginal increase in areal density of approximately 4%.

Mohammad and colleagues [178] grew ZnO nanowires on aramid fabrics and, through impact tests at velocities of 22–40 m/s, demonstrated an improvement of about 66% in impact resistance due to increased inter-yarn friction, without compromising flexibility or adding significant weight, highlighting the method's potential for use in soft armors. Kelsey

Steinke et al. [179] treated UHMWPE fabrics with oxygen plasma to facilitate ZnO nanowire growth via a hydrothermal process. The results revealed major improvements in inter-yarn friction and pull-out energy (up to +822.9%), along with significant enhancements in ballistic performance (V_{50} by +59.1% and absorbed impact load by +227%), demonstrating the strong potential of this method for UHMWPE-based ballistic armor.

Table 2 summarizes the main types of nanostructured coatings investigated for ballistic textiles, highlighting their specific contributions to enhanced mechanical and protective properties, along with representative studies from the literature.

Table 2. Coating strategies and their impact on the mechanical and ballistic properties of protective textiles.

Coating Type	Uncoated Baseline Material	Improved Property	Ref.
Nanosilica (STF impregnation and surface coatings)	Kevlar KM2, Kevlar fabrics, Twaron	Increased energy absorption, higher inter-yarn friction, improved puncture and ballistic resistance, preserved flexibility	[48,137,138]
Graphene/Graphene Oxide (GO)	Kevlar KM2, Kevlar XP, para-aramid fabrics	Enhanced tensile strength and toughness, improved interfacial adhesion, higher absorbed energy (up to +50%), reduced number of layers required, increased thermal stability	[5,75,147–151]
Laser-Induced Graphene (LIG)	Cotton fabric and polyamide fabric (depending on study)	Improved energy absorption, EMI shielding efficiency (~50 dB), multifunctionality (self-sensing and impact detection)	[156,157]
Carbon Nanotubes (CNTs)	Kevlar KM2 and Twaron CT747	Increased tensile strength (up to +46%), improved inter-yarn friction, higher ballistic limit (+50%), energy absorption (+240%), multifunctional capabilities (smart textiles)	[168–173]
ZnO Nanowires	Kevlar KM2 and Twaron fabrics	Enhanced inter-yarn friction, higher pull-out energy (+822.9%), improved impact resistance (+66%), increased ballistic performance (V_{50} +59.1%), with negligible weight increase	[176–178]

As shown in Table 2, different nanostructured coatings, such as nanosilica-based shear-thickening fluids, graphene and graphene oxide layers, laser-induced graphene, carbon nanotubes, and zinc oxide nanowires, have been demonstrated to significantly improve the performance of ballistic textiles, each material conferring specific advantages ranging from increased inter-yarn friction, tensile strength, absorbed energy, and ballistic limit, to multifunctional capabilities such as EMI shielding and self-sensing, thereby highlighting the potential of advanced coatings to simultaneously enhance protection efficiency and introduce additional functionalities without compromising the lightweight and flexible nature of the fabrics.

Across the literature, various coating methods (dip coating, sol–gel, ultrasonication, vacuum filtration, hydrothermal growth, STF impregnation) and functional materials (TiO_2/ZnO, SiO_2-STF, fumed silica, GO, MWNT/CNT-STF, ZnO nanowires) have been applied to Kevlar and Twaron fabrics (Table 3). Reported ballistic improvements range from +35% to +200% in impact resistance, up to +50% in ballistic limit, and up to +985% in yarn pull-out resistance. The dominant enhancement mechanisms include increased inter-yarn friction, mechanical interlocking, shear-thickening stiffening, surface roughening, restricted yarn mobility, and improved load transfer, all contributing to higher energy absorption and reduced yarn slippage under impact.

Table 3. Comparative summary of coating strategies for enhanced ballistic performance.

Coating Methods	Coating Materials	Substrate	Reported Ballistic Improvement	Mechanism of Enhancement	Ref.
Dip–Pad–Dry method (sol–gel method)	TiO_2/ZnO hydrosols (submicrometric vs. nanometric particles)	Twaron aramid fibers	CSF = 0.1617 and CKF = 0.1554; Tensile strength reduction < 10%; Reduction in strain and modulus < 5%; Weight increase ~4% without curing; ≈0% or slight decrease with curing.	Rougher surface with "lump-like" features (submicron) or "film-like" coating (nano); Improved ballistic performance potential.	[105]
	TiO_2/ZnO submicron hydrosol	Twaron® yarns and fabric	Inter-yarn friction increased by more than 20%, with the CSF 0.1991 and the CKF 0.1871; The energy absorption increased by more than 35% under impact velocities of 450–500 m/s.	A significantly rougher yarn surface, forming lump-like structures that enhanced mechanical interlocking between yarns; Higher ballistic energy absorption.	[106]
Soaking method	SiO_2 NPs 500 nm (15, 25, 35, and 45 wt.%) in polyethylene glycol (PEG)	Kevlar fabrics (2- and 4-layers)	STF impregnation increased energy absorption; 35 wt.% nanosilica yielded the highest specific energy absorption; Ballistic resistance improved from 15 to 35 wt.% nanosilica; Only marginal improvement from 35 to 45 wt.%; Pull-out force increased consistently with higher nanoparticle content.	Improved impact resistance, reduced yarn pull-out, and more efficient multilayer interaction during impact.	[48]
	STFs were prepared by dispersing fumed silica nanoparticles	Aramid fabrics Twaron TM (CT709)	Higher silica loading increased stab and ballistic resistance, with 30% SiO_2 giving the best overall performance; At this concentration, the shear-thickening response was maximized, stab resistance improved the most, and penetration resistance of STF-impregnated aramid also reached its peak.	Silica-based STFs enhance energy absorption and penetration resistance; higher silica loading strengthens shear thickening, enabling rapid impact stiffening and better protection.	[139]
Coating method	Modified SiO_2 NPs in PVB/ethanol sol	p-aramid fiber type Twaron	Stopped all bullets; only back-face deformation observed.	Nanosilica stiffening, better energy dissipation, reduced yarn pull-out.	[138]
Vacuum filtration method	Graphene oxide (GO)	Twaron® textile	The ballistic resistance of the aramid fabric increases with the deposition of GO by values up to 50% higher than those for the as-received fabric.	Increase in ballistic resistance.	[152]

Table 3. *Cont.*

Coating Methods	Coating Materials	Substrate	Reported Ballistic Improvement	Mechanism of Enhancement	Ref.
Impregnation method	CNT/PSt-EA-based shear-thickening fluid (C-STF)	Kevlar plain-weave fabric	Ballistic limit improved from 84.6 m/s to 96.5 m/s with C-STF impregnation; Optimum CNT content (1.0%) increased V_{50} to 96.5 m/s; excessive CNT reduced performance; Increasing STF dispersed-phase volume (53.5% to 58.5%) raised V_{50} from 92.9 to 99.5 m/s.	Increased inter-yarn friction and enlarged bearing area due to C-STF doping, improving energy dissipation and impact resistance.	[168]
Ultrasonication-assisted treatment method	MWNTs dispersed in N-methyl-2-pyrrolidone (NMP)	Kevlar K129 yarns and Kevlar K129 fabrics	50% increase in ballistic limit with MWNT treatment (mass increase only 0.4–1.4%).	MWNT coating increases fiber–fiber interaction and friction, enhancing energy transfer and reducing yarn pull-out at impact.	[170]
"soak and dry" method	STF based on SiO_2 nanoparticles (71 wt%) dispersed in PEG 200 STF with various loadings (15%, 55%, 75%)	Kevlar fabric	STF-15%/Kevlar showed 200% improvement in impact resistance; STF-55%/Kevlar showed superior puncture resistance versus neat Kevlar; STF/Kevlar (15%, 55%, 75%) outperformed neat Kevlar at all energies tested (8.6–17.2 J); STF/Kevlar penetration depth significantly decreased with increasing STF content.	Higher STF viscosity increases inter-yarn friction and impact stiffening, forming a viscous network that improves load transfer and reduces penetration, while PEG alone acts as a lubricant, confirming friction enhancement as the key protection mechanism.	[171]
Dip coating (3×) + hydrothermal ZnO nanowire growth	ZnO nanoparticles + ZnO nanowires	Aramid (Kevlar) fabric	Elastic modulus increased by 8.8% (from 61.88 to 67.36 GPa). Tensile strength increased by 13.2% (≈2.49 GPa); Peak impact load increased from 1268 N to 2107 N (≈66%); Prevention of projectile penetration in the 30–34 m/s window; Yarn pull-out resistance increased (up to +985% at peak pull-out load).	Increased fiber and yarn friction; Limited yarn mobility; nanowires fill crossovers; Enhanced surface roughness; Improved load transfer and energy dissipation.	[178]

3.3. Economic and Scalability Considerations for Coating Materials and Processes

In addition to performance, the economic viability and industrial scalability of coating materials are essential for their practical implementation in ballistic protection systems. Silica nanoparticles, PEG, PVB, and sol–gel precursors are low cost and widely available, making nanosilica-based STFs and sol–gel coatings economically attractive for large-scale production. In contrast, graphene oxide, CNTs, and ZnO nanowires involve higher material costs and more energy-intensive processing routes such as vacuum filtration or hydrothermal growth, which limits their use to specialized applications where maximum performance is required.

From a manufacturing perspective, dip-coating, soaking, pad–dry–cure, and sol–gel routes are compatible with existing textile finishing lines and thus offer excellent scalability and low processing costs. Methods such as ultrasonic-assisted treatment, aerosol deposition, or hydrothermal nanowire growth present higher complexity and processing costs, making them less suitable for the mass production of soft armor systems. Considering these aspects, the selection of coating systems should be guided by heuristic criteria, including the cost–performance ratio, added areal density, processing time and energy consumption, equipment requirements, durability, and compatibility with standard textile technologies. The inclusion of these factors enables a realistic assessment of the translational potential of each coating system.

Although current coating strategies ranging from nanosilica-based STFs and graphene/GO layers to CNT- and ZnO nanowire-modified fabrics have demonstrated substantial improvements in ballistic performance, several challenges remain and define important directions for future research.

Although individual nanocoatings such as nanosilica-based STFs, CNT networks, graphene derivatives, and ZnO nanowires have been extensively studied, hybrid nanocoating systems remain comparatively underexplored in the ballistic domain. A few recent works demonstrate the potential of multi-component interfaces—for example, para-aramid fabrics modified with hybrid B_4C/MWCNT/graphene nanoplatelet coatings showing enhanced pull-out and interfacial behavior [180] or graphene–CNT hybrid coatings that improve fiber–matrix adhesion in composite architectures [181]. Other studies report ZnO–graphene hybrid structures on textile or flexible substrates, evidencing synergistic effects between 1D and 2D nanomaterials in terms of mechanical anchoring, load transfer, and stress distribution [182,183]. Hybrid rGO/ZnO systems or ZnO–AgNW–graphene coatings on fabrics further highlight the benefits of hierarchical nano-interfaces [182,184], while graphene oxide–Fe_3O_4 hybrid nanofillers incorporated in STF formulations demonstrate improved yarn pull-out and impact responses in Kevlar systems [185]. Despite these promising examples, systematic investigations addressing how such hybrid nanoscale architectures influence inter-yarn friction, energy absorption, coating durability, and multi-hit ballistic behavior remain scarce. This gap underscores the need for controlled studies on synergistic versus competitive interactions between 1D nanostructures and 2D nanomaterials applied to the same fiber surface.

A key issue is the long-term durability and stability of coatings under realistic service conditions, including humidity, sweat, UV exposure, repeated flexing, washing, and multi-hit impact scenarios, where debonding, microcracking, or loss of functionality may occur. For STF-based systems, preventing particle sedimentation, phase separation, or leakage from the fabric over time remains a critical concern, as does maintaining flexibility and comfort while achieving sufficient stiffening under impact. For nanostructured coatings such as CNTs, graphene, and ZnO nanowires, open questions include optimizing interfacial adhesion, controlling nanomaterial dispersion and alignment on complex textile architectures, and ensuring user safety and environmental compatibility.

While durability issues are briefly introduced above, a more systematic assessment of degradation mechanisms affecting nanocoating adhesion on ballistic textiles is critically needed. UV radiation can induce chain scission in polymeric binders, oxidize graphene-based layers, and weaken silane coupling interfaces, ultimately reducing coating–fiber adhesion and increasing brittleness. Sweat exposure introduces salts, lactic acid, and variable pH conditions that can disrupt hydrogen bonding, accelerate hydrolysis of sol–gel networks, or corrode metal-oxide nanostructures, leading to gradual delamination or loss of conductivity. Repeated flexing imposes cyclic shear and bending stresses at the coating–fiber interface; brittle or poorly anchored nanostructures such as ZnO nanowires or thick graphene stacks may develop microcracks, breakage, or particle shedding, thereby altering frictional behavior and energy absorption. Chemical agents, including detergents, alcohols, oils, and cleaning solvents, may swell polymer matrices, dissolve weakly bound layers, or change surface energy, compromising wettability and interfacial adhesion. Despite these known degradation pathways, systematic studies quantifying the combined effects of UV, perspiration chemistry, laundering cycles, and mechanical fatigue on nanocoating adhesion remain scarce. Existing reports tend to provide anecdotal or single-factor evaluations, underscoring a significant research gap. Comprehensive, standardized durability protocols, including accelerated aging, UV–sweat synergies, cyclic flexing under controlled humidity, and post-aging ballistic testing, are essential for translating laboratory-developed coatings into field-ready ballistic textile systems.

From a design standpoint, there is still a need for standardized testing protocols that directly link coating architecture, inter-yarn friction, and multi-layer panel response to specific ballistic threats. Promising research opportunities lie in the development of multifunctional coatings that combine ballistic enhancement with sensing, EMI shielding, thermal management, or self-healing capabilities, as well as in the integration of advanced multiscale modeling tools to guide coating design and accelerate the translation of laboratory concepts into deployable, field-ready ballistic systems.

It is important to note that, despite the growing interest in advanced coating technologies for ballistic protection, the scientific literature does not yet provide quantitative cost data for most nanostructured coating materials (e.g., graphene derivatives, CNT networks, ZnO nanowires, nano-ceramic layers, or STF formulations). Comprehensive cost–benefit analyses are currently absent from peer-reviewed studies, primarily because ballistic survivability, reliability, and impact performance remain the dominant priorities at this stage of technology development. Additionally, confidentiality constraints related to defense applications and the early-stage maturity of many nanocoating techniques limit the availability of transparent pricing structures or standardized economic benchmarks. Consequently, while qualitative assessments of relative cost levels and scalability can be made, precise quantitative economic metrics cannot yet be reported based on the existing literature.

4. Conclusions

This review has shown that the evolution of ballistic protection systems has been strongly influenced by advances in both bulk materials and functional surface coatings. Metals, ceramics, polymers, and composites continue to serve as the fundamental building blocks of armor systems, yet their intrinsic limitations in terms of weight, flexibility, or multi-impact performance have stimulated the search for innovative strategies. Coatings based on nanosilica, graphene and its derivatives, carbon nanotubes (CNTs), and zinc oxide nanowires (ZnO NWs) have emerged as promising approaches, offering significant improvements in interfacial adhesion, inter-yarn friction, impact energy absorption, and overall ballistic performance. Results from experimental investigations and numerical simulations consistently confirm that such nanostructured coatings enhance ballistic limit

velocity, reduce the back-face signature, and enable higher levels of protection at lower areal density, thus contributing to lighter and more effective armor.

Beyond the mechanical improvements, recent studies highlight the multifunctional potential of advanced coatings. CNT and laser-induced graphene (LIG)-based layers not only strengthen protective performance but also introduce added functionalities such as electrical conductivity, in situ impact sensing, EMI shielding, and enhanced thermal stability. These developments indicate a paradigm shift toward smart and adaptive protective textiles capable of both resisting threats and monitoring structural health.

Future perspectives emphasize the need for scalable, cost-effective, and environmentally sustainable coating processes to enable industrial implementation. Research efforts should focus on optimizing nanoparticle dispersion, controlling coating thickness and uniformity, and ensuring long-term durability under real operational conditions such as humidity, temperature fluctuations, and repeated impacts. Hybrid systems that combine multiple nanomaterials, such as graphene with CNTs or ZnO nanowires with nanosilica, represent another promising direction, as synergistic effects may further enhance energy dissipation and multifunctionality. Additionally, integrating advanced modeling and simulation tools, such as finite element analysis and molecular dynamics, with experimental testing will accelerate the design of optimized coating–substrate systems.

Overall, coating technologies offer a versatile and highly effective pathway for the development of next-generation ballistic textiles. By merging lightweight design, enhanced impact resistance, and multifunctional capabilities, future protective systems are expected to address the increasingly complex challenges of modern defense and security, paving the way for more adaptable, durable, and intelligent armor solutions.

This review highlights that one of the persistent challenges in ballistic protection is the fundamental tradeoff between achieving high resistance to sharp or high-velocity impact and maintaining the low weight and flexibility required for user comfort and mobility. Although current materials offer excellent strength-to-weight ratios, improvements in ballistic efficiency often come with penalties in stiffness or mass. The coating-based strategies and material concepts discussed herein specifically target this research gap, demonstrating that interfacial engineering, nanoparticle reinforcement, and hybrid multilayer architectures can enhance energy absorption and penetration resistance while mitigating the traditional compromises associated with armor design.

Despite these promising advances, several challenges remain. Ensuring long-term durability, uniform nanoparticle dispersion, coating stability under humidity and temperature cycling, and maintaining flexibility without sacrificing protection are key issues that require further study. Future opportunities lie in scalable and cost-efficient coating routes, hybrid nanomaterial systems with synergistic energy dissipation mechanisms, and integrating sensing or multifunctional capabilities into protective layers. Addressing these aspects will accelerate the translation of coated ballistic textiles from laboratory development to reliable field applications.

Author Contributions: Conceptualization, G.G.A. and D.L.B.; methodology, G.B.C.; validation, T.V.T.; investigation, G.B.C. and T.V.T.; resources, G.G.A. and D.L.B.; writing—original draft preparation, G.G.A. and D.L.B.; writing—review and editing, D.L.B. All authors have read and agreed to the published version of the manuscript.

Funding: This research was funded by "Dunarea de Jos" University of Galati, Romania, grant research no. 7954/31.03.2025.

Informed Consent Statement: The current review is limited to the field of materials science and surface engineering. The research discussed is beneficial for the development of advanced protective coatings and composite systems for civilian safety and industrial applications and does not pose

any threat to public health or national security. The authors acknowledge the theoretical dual-use potential of research involving ballistic protection materials and confirm that all necessary precautions have been taken to prevent potential misuse. The authors strictly adhere to relevant national and international regulations regarding dual-use research and advocate for responsible deployment, ethical considerations, regulatory compliance, and transparent reporting.

Data Availability Statement: All data analyzed during this study are included in this published article.

Acknowledgments: This research was supported by Doctoral School of Fundamental Sciences and Engineering, Materials Engineering domain of "Dunarea de Jos" University of Galati, Romania.

Conflicts of Interest: The authors declare no conflicts of interest.

References

1. Chen, X. (Ed.) *Advanced Fibrous Composite Materials for Ballistic Protection*; Woodhead Publishing: Cambridge, UK, 2016. [CrossRef]
2. Strelko, O.; Horban, A. Analysis of the History of Creation and Improvement of Personal Protective Equipment: From Bronze Armor to Modern Bulletproof Vests. *Hist. Sci. Technol.* **2023**, *13*, 201–222. [CrossRef]
3. Yi, R.-C.; Yin, L.-K.; Wang, J.-R.; Chen, Z.-G.; Hu, D.-Q. Study on the Performance of Ceramic Composite Projectile Penetrating into Ceramic Composite Target. *Def. Technol.* **2017**, *13*, 295–299. [CrossRef]
4. Sitotaw, D.B.; Ahrendt, D.; Kyosev, Y.; Kabish, A.K. A Review on the Performance and Comfort of Stab Protection Armor. *Autex Res. J.* **2021**, *21*, 255–272. [CrossRef]
5. David, N.V.; Gao, X.-L.; Zheng, J.Q. Ballistic Resistant Body Armor: Contemporary and Prospective Materials and Related Protection Mechanisms Available to Purchase. *Appl. Mech. Rev.* **2009**, *62*, 050802. [CrossRef]
6. Haro, E.E.; Szpunar, J.A.; Odeshi, A.G. Ballistic Impact Response of Laminated Hybrid Materials Made of 5086-H32 Aluminum Alloy, Epoxy and Kevlar Fabrics Impregnated with Shear Thickening Fluid. *Compos. Part A Appl. Sci. Manuf.* **2016**, *87*, 54–65. [CrossRef]
7. Abtew, M.A.; Boussu, F.; Bruniaux, P.; Loghin, C.; Cristian, I. Ballistic Impact Mechanisms—A Review on Textiles and Fibre-Reinforced Composites Impact Responses. *Compos. Struct.* **2019**, *223*, 110966. [CrossRef]
8. Yavaş, M.O.; Avcı, A.; Şimşir, M.; Akdemir, A. Ballistic Performance of Kevlar49/UHMW-PEHB26 Hybrid Layered Composite. *Int. J. Eng. Res. Dev.* **2015**, *7*, 21–27. [CrossRef]
9. Erlich, D.C.; Shockey, D.A.; Simons, J.W. Slow Penetration of Ballistic Fabrics. *Text. Res. J.* **2003**, *73*, 179–184. [CrossRef]
10. Zahid, B.; Chen, X. Impact Performance of Single-Piece Continuously Textile Reinforced Riot Helmet Shells. *J. Compos. Mater.* **2014**, *48*, 761–776. [CrossRef]
11. Azmi, M.R.; Sultana, M.T.H.; Hamdan, A.; Nor, A.F.M.; Jayakrishna, K. Flexural and Impact Properties of a New Bulletproof Vest Insert Plate Design Using Kenaf Fibre Embedded with X-Ray Films. *Mater. Today Proc.* **2018**, *5*, 11193–11197. [CrossRef]
12. Yang, Y.; Chen, X. Investigation of Energy Absorption Mechanisms in a Soft Armor Panel under Ballistic Impact. *Text. Res. J.* **2017**, *87*, 2475–2486. [CrossRef]
13. Zohdi, T.I. Modeling and Simulation of Progressive Penetration of Multilayered Ballistic Fabric Shielding. *Comput. Mech.* **2002**, *29*, 61–67. [CrossRef]
14. Joo, K.; Kang, T.J. Numerical Analysis of Energy Absorption Mechanism in Multi-Ply Fabric Impacts. *Text. Res. J.* **2008**, *78*, 561–576. [CrossRef]
15. Karahan, M.; Kuş, A.; Eren, R. An Investigation into Ballistic Performance and Energy Absorption Capabilities of Woven Aramid Fabrics. *Int. J. Impact Eng.* **2008**, *35*, 499–510. [CrossRef]
16. Liu, J.; Long, Y.; Ji, C.; Liu, Q.; Zhong, M.; Zhou, Y. Influence of Layer Number and Air Gap on the Ballistic Performance of Multi-Layered Targets Subjected to High Velocity Impact by Copper EFP. *Int. J. Impact Eng.* **2018**, *112*, 52–65. [CrossRef]
17. Stupar, S. Ballistic Composites, the Present and the Future. In *Smart and Advanced Ceramic Materials and Applications*; IntechOpen: London, UK, 2022. [CrossRef]
18. *NIJ 0101.06/0101.07*; Ballistic Resistance of Body Armor. U.S. Department of Justice: Washington, DC, USA, 2023.
19. *NATO AEP-55/STANAG 4569*; Protection Levels for Occupants of Logistic and Light Armoured Vehicles. NATO Standardization Office: Brussels, Belgium, 2005.
20. Balos, S.; Howard, D.; Brezulianu, A.; Labus Zlatanović, D. Perforated Plate for Ballistic Protection—A Review. *Metals* **2021**, *11*, 526. [CrossRef]
21. Savić, B.; Cabrilo, A. Effect of Heat Input on the Ballistic Performance of Armor Steel Weldments. *Materials* **2021**, *14*, 3617. [CrossRef]
22. Khan, W.; Tufail, M.; Chandio, A.D. Characterization of Microstructure, Phase Composition, and Mechanical Behavior of Ballistic Steels. *Materials* **2022**, *15*, 2204. [CrossRef]

23. Trajkovski, J.; Kunc, R.; Pepel, V.; Prebil, I. Flow and Fracture Behavior of High-Strength Armor Steel PROTAC 500. *Mater. Des.* **2015**, *66*, 37–45. [CrossRef]
24. Nicolescu, C.; Tiganescu, T.V.; Antoniac, A.; Iorga, O.; Ghiban, B.; Pascu, A.; Streza, A.; Antoniac, I. Mechanical Properties and Ballistic Performance for Different Coatings on HARDOX 450 Steel for Defense Applications. *Crystals* **2025**, *15*, 687. [CrossRef]
25. Vilíš, J.; Kosiuczenko, K.; Nowakowski, M.; Tupaj, M.; Trytek, A.; Zouhar, J.; Vítek, R.; Gregor, L.; Pokorný, Z. Comprehensive Evaluation of Layered Composite Protection Performance for Light Armored Vehicles. *J. Mater. Eng. Perform.* **2025**. [CrossRef]
26. Acar, D.; Canpolat, B.H.; Cora, Ö.N. Ballistic Performances of Ramor 500, Armox Advance and Hardox 450 Steels under Monolithic, Double-Layered, and Perforated Conditions. *Eng. Sci. Technol. Int. J.* **2024**, *51*, 101653. [CrossRef]
27. Appleby-Thomas, G.J.; Wood, D.C.; Hameed, A.; Painter, J.; Fitzmaurice, B. On the Effects of Powder Morphology on the Post-Comminution Ballistic Strength of Ceramics. *Int. J. Impact Eng.* **2017**, *100*, 46–55. [CrossRef]
28. Pittari, J.; Subhash, G.; Zheng, J.; Halls, V.; Jannotti, P. The Rate-Dependent Fracture Toughness of Silicon Carbide- and Boron Carbide-Based Ceramics. *J. Eur. Ceram. Soc.* **2015**, *35*, 4411–4422. [CrossRef]
29. Bresciani, L.M.; Manes, A.; Giglio, M. An Analytical Model for Ballistic Impacts against Ceramic Tiles. *Ceram. Int.* **2018**, *44*, 21249–21261. [CrossRef]
30. Boldin, M.S.; Berendeev, N.N.; Melekhin, N.V.; Popov, A.A.; Nokhrin, A.V.; Chuvildeev, V.N. Review of Ballistic Performance of Alumina: Comparison of Alumina with Silicon Carbide and Boron Carbide. *Ceram. Int.* **2021**, *47*, 25201–25213. [CrossRef]
31. Fortini, J.I.N.; Da Silveira, P.H.P.M.; Monteiro, S.N.; Pereira, A.S.; Lima, E.S. Mechanical, Microstructural Properties and Ballistic Performance of SiC/Si Ceramics against 5.56 × 45 mm Projectile. *J. Mater. Res. Technol.* **2025**, *35*, 208–219. [CrossRef]
32. Chauhan, A.; Schaefer, M.C.; Haber, R.A.; Hemker, K.J. Experimental Observations of Amorphization in Stoichiometric and Boron-Rich Boron Carbide. *Acta Mater.* **2019**, *181*, 207–215. [CrossRef]
33. Charalambous, H.; Yang, Q.; Rivera, J.; Crystal, I.R.; Sun, L.Y.; Thorpe, F.; Rosenberg, W.; McCormack, S.J.; King, G.C.S.; Cahill, J.T.; et al. Thermostructural Evolution of Boron Carbide Characterized Using In-Situ X-Ray Diffraction. *Acta Mater.* **2024**, *265*, 119597. [CrossRef]
34. Gilson, L.; Rabet, L.; Imad, A.; Coghe, F.; Van Roey, J.; Guéders, C.; Gallant, J. Ballistic Impact Response of an Alumina-Based Granular Material: Experimental and Numerical Analyses. *Powder Technol.* **2021**, *385*, 273–286. [CrossRef]
35. Yang, S.; Lu, L.; Gao, Y.; Zhang, Y.; Wang, T.; Liu, Z. Experimental and Theoretical Study of Cone Angle in Alumina Tiles under Ballistic Impact. *Int. J. Impact Eng.* **2024**, *192*, 105025. [CrossRef]
36. He, Y.; Jia, N.; Zhou, J.Q.; Jiao, Y.; Lei, H. Designing SiC Ceramic Composite Armor Structure to Resist Multiple Impacts from Armor-Piercing Incendiary Bullets. *Int. J. Impact Eng.* **2025**, *203*, 105367. [CrossRef]
37. *NIJ 0123.00*; Specification for NIJ Ballistic Protection Levels and Associated Test Threats. National Institute of Justice, U.S. Department of Justice: Washington, DC, USA, 2023.
38. Xu, D.; Huang, Z.; Chen, G.; Ren, X.; Li, D.; Zhang, Y.; Li, Y. Experimental Investigation on the Ballistic Performance of B4C/Aramid/UHMWPE Composite Armors against API Projectile under Different Temperatures. *Thin-Walled Struct.* **2024**, *196*, 111553. [CrossRef]
39. Zhang, Y.; Dong, H.; Liang, K.; Huang, Y. Impact Simulation and Ballistic Analysis of B4C Composite Armour Based on Target Plate Tests. *Ceram. Int.* **2021**, *47*, 10035–10049. [CrossRef]
40. Wang, Y.; Liu, Q.; Zhang, B.; Wang, H.; Hazell, P.J.; Han, Z.; Li, J.; Li, B.; Li, L.; Liu, F.; et al. Ballistic Performance of Functionally Graded B4C/Al Composites without Abrupt Interfaces: Experiments and Simulations. *J. Mater. Res. Technol.* **2023**, *25*, 1011–1029. [CrossRef]
41. Shaker, K.; Nawab, Y. Fibers for Protective Textiles. In *Fibers for Technical Textiles*; Springer: Singapore, 2020; pp. 65–91. [CrossRef]
42. Tam, D.K.Y.; Ruan, S.; Gao, P.; Yu, T. High-Performance Ballistic Protection Using Polymer Nanocomposites. In *Advances in Military Textiles and Personal Equipment*; Sparks, E., Ed.; Woodhead Publishing: Cambridge, UK, 2012; pp. 213–237. [CrossRef]
43. Kwolek, S.L. Chemical Heritage Foundation, 2015. Available online: http://www.chemheritage.org/discover/online-resources/chemistry-in-history/themes/petrochemistry-and-synthetic-polymers/synthetic-polymers/kwolek.aspx (accessed on 23 May 2025).
44. Protyai, M.I.H.; Adib, F.M.; Taher, T.I.; Karim, M.R.; Rashid, A.B. Performance Evaluation of Kevlar Fiber Reinforced Epoxy Composite by Depositing Graphene/SiC/Al_2O_3 Nanoparticles. *Hybrid Adv.* **2024**, *6*, 100245. [CrossRef]
45. DuPont. Kevlar® Aramid Fiber. DuPont Romania, 2015. Available online: http://www.dupont.com/products-and-services/fabrics-fibers-nonwovens/fibers/brands/kevlar.html (accessed on 23 May 2025).
46. He, Q.; Cao, S.; Wang, Y.; Xuan, S.; Wang, P.; Gong, X. Impact Resistance of Shear Thickening Fluid/Kevlar Composite Treated with Shear-Stiffening Gel. *Compos. Part A Appl. Sci. Manuf.* **2018**, *106*, 82–90. [CrossRef]
47. Khodadadi, A.; Liaghat, G.; Vahid, S.; Sabet, A.R.; Hadavinia, H. Ballistic Performance of Kevlar Fabric Impregnated with Nanosilica/PEG Shear Thickening Fluid. *Compos. Part B Eng.* **2019**, *162*, 643–652. [CrossRef]
48. Park, J.L.; Yoon, B.I.; Paik, J.G.; Kang, T.J. Ballistic Performance of P-Aramid Fabrics Impregnated with Shear Thickening Fluid; Part I—Effect of Laminating Sequence. *Text. Res. J.* **2012**, *82*, 527–541. [CrossRef]

49. Wang, Y.; Li, S.K.; Feng, X.Y. The Ballistic Performance of Multi-Layer Kevlar Fabrics Impregnated with Shear Thickening Fluids. *Adv. Mater. Res.* **2015**, *782*, 153–157. [CrossRef]
50. Sen, S.; Jamal, N.B.; Shaw, A.; Deb, A. Numerical Investigation of Ballistic Performance of Shear Thickening Fluid (STF)-Kevlar Composite. *Int. J. Mech. Sci.* **2019**, *164*, 105174. [CrossRef]
51. Brown, E.; Jaeger, H.M. Shear Thickening in Concentrated Suspensions: Phenomenology, Mechanisms and Relations to Jamming. *Rep. Prog. Phys.* **2014**, *77*, 046602. [CrossRef]
52. Egres, R.G.; Wagner, N.J. The Rheology and Microstructure of Acicular Precipitated Calcium Carbonate Colloidal Suspensions through the Shear Thickening Transition. *J. Rheol.* **2005**, *49*, 719–746. [CrossRef]
53. Liao, J.B.; Wen, H.M. A Constitutive Model for Shear Thickening Fluid (STF) Impregnated Kevlar Fabric Subjected to Impact Loading. *Int. J. Impact Eng.* **2024**, *191*, 104990. [CrossRef]
54. Chen, Q.; Liu, M.; Xuan, S.; Jiang, W.; Cao, S.; Gong, X. Shear Dependent Electrical Property of Conductive Shear Thickening Fluid. *Mater. Des.* **2017**, *121*, 92–100. [CrossRef]
55. Bosco, A.; Paiva, F.; Odenbach, S.; Calado, V. Influence of Particle Shape and Sample Preparation on Shear Thickening Behavior of Precipitated Calcium Carbonate Suspensions. *Adv. Powder Technol.* **2021**, *32*, 802–809. [CrossRef]
56. Zheng, S.B.; Xuan, S.H.; Jiang, W.Q.; Gong, X.L. High Performance Shear Thickening Fluid Based on Calcinated Colloidal Silica Microspheres. *Smart Mater. Struct.* **2015**, *24*, 085033. [CrossRef]
57. Gürgen, S.; Kuşhan, M.C. The Stab Resistance of Fabrics Impregnated with Shear Thickening Fluids Including Various Particle Size of Additives. *Compos. Part A Appl. Sci. Manuf.* **2017**, *94*, 50–60. [CrossRef]
58. Xie, Z.; Liu, Y.; Liu, L.; Feng, R.; Jiang, W.; Chen, W. Research on the Adaptability of STF-Kevlar to Ambient Temperature under Low-Velocity Impact Conditions. *Polym. Test.* **2024**, *133*, 108416. [CrossRef]
59. Xie, Z.; Chen, W.; Liu, Y.; Liu, L.; Zhao, Z.; Luo, G. Design of the Ballistic Performance of Shear Thickening Fluid (STF) Impregnated Kevlar Fabric via Numerical Simulation. *Mater. Des.* **2023**, *226*, 111599. [CrossRef]
60. Ma, Y.; Hong, X.; Lei, Z.; Bai, R.; Liu, Y.; Yang, J. Shear Response Behavior of STF/Kevlar Composite Fabric in Picture Frame Test. *Polym. Test.* **2022**, *113*, 107652. [CrossRef]
61. Tang, E.; Hou, J.; Wang, R.; Han, Y.; Chen, C.; Chang, M.; Guo, K.; He, L. Energy Absorption Characteristics of STF Impregnated Kevlar Fabric Coating GFRP Composite Structure by Projectile High-Velocity Impact. *Polym. Test.* **2024**, *140*, 108596. [CrossRef]
62. Wang, X.; Li, J.; Yu, J.; Li, M.; Li, R.; He, Z.; Dong, J.; Wang, P.; Chen, Y.; Yang, X.; et al. The Effect of STF-Kevlar Composite Materials on the Impact Response of Fibre Metal Laminates. *Compos. Commun.* **2024**, *48*, 101936. [CrossRef]
63. Alexe, F.; Sau, C.; Iorga, O.; Toader, G.; Diacon, A.; Rusen, E.; Lazaroaie, C.; Ginghina, R.E.; Tiganescu, T.V.; Teodorescu, M.; et al. Experimental Investigations on Shear Thickening Fluids as "Liquid Body Armors": Non-Conventional Formulations for Ballistic Protection. *Polymers* **2024**, *16*, 2305. [CrossRef]
64. Russell, B.P.; Karthikeyan, K.; Deshpande, V.S.; Fleck, N.A. The High Strain Rate Response of Ultra High Molecular-Weight Polyethylene: From Fibre to Laminate. *Int. J. Impact Eng.* **2013**, *60*, 1–9. [CrossRef]
65. Malito, L.G.; Arevalo, S.; Kozak, A.; Spiegelberg, S.; Bellare, A.; Pruitt, L. Material Properties of Ultra-High Molecular Weight Polyethylene: Comparison of Tension, Compression, Nanomechanics and Microstructure across Clinical Formulations. *J. Mech. Behav. Biomed. Mater.* **2018**, *83*, 9–19. [CrossRef]
66. Kurtz, S.M. (Ed.) *UHMWPE Biomaterials Handbook: Ultra High Molecular Weight Polyethylene in Total Joint Replacement and Medical Devices*; Academic Press: Cambridge, MA, USA, 2009.
67. Elkarem, A.H. A Study on Dyneema Fabric for Soft Body Armor. *Int. J. Eng. Appl. Sci. Technol.* **2020**, *5*, 115–121. [CrossRef]
68. Bian, J.; Dai, K.; Lv, X.; Huang, Z.; Wu, G.; Zhang, Y. Effect of Material and Structure of Ultra-High-Molecular-Weight Polyethylene Body Armor on Ballistic Limit Velocity: Numerical Simulation. *Polymers* **2024**, *16*, 2985. [CrossRef]
69. Karahan, M. Comparison of Ballistic Performance and Energy Absorption Capabilities of Woven and Unidirectional Aramid Fabrics. *Text. Res. J.* **2008**, *78*, 718–730. [CrossRef]
70. Effendi, N.M.; Sastranegara, A.; Hernawan, R.; Anggraini, L. Impact Behavior of Multi-Layered UHMWPE Vests Reinforced with Titanium and PVC for Ballistic Protection. *Indones. J. Comput. Eng. Des. (IJoCED)* **2025**, *7*, 61–73. [CrossRef]
71. Gao, Y.; Feng, X.; Liu, J.; Fu, H.; Li, S.; He, C. Design and Ballistic Penetration of "SiC/Ti6Al4V/UHMWPE" Composite Armor. *IOP Conf. Ser. Mater. Sci. Eng.* **2019**, *563*, 042009. [CrossRef]
72. Pundhir, N.; Pathak, H.; Zafar, S. Ballistic Impact Performance of Ultra-High Molecular Weight Polyethylene (UHMWPE) Composite Armour. *Sādhanā* **2021**, *46*, 194. [CrossRef]
73. Chinnasamy, V.; Subramani, S.P.; Palaniappan, S.K.; Mylsamy, B.; Aruchamy, K. Characterization on Thermal Properties of Glass Fiber and Kevlar Fiber with Modified Epoxy Hybrid Composites. *J. Mater. Res. Technol.* **2020**, *9*, 3158–3167. [CrossRef]
74. Biradar, A.; Arulvel, S.; Kandasamy, J.; Sultan, M.T.H.; Shahar, F.S.; Najeeb, M.I.; Gaff, M.; Hui, D. Nanocoatings for Ballistic Applications: A Review. *Nanotechnol. Rev.* **2023**, *12*, 20230574. [CrossRef]
75. Gu, H.; Liu, C.; Zhu, J.; Gu, J.; Wujcik, E.K.; Shao, L.; Wang, N.; Wei, H.; Scaffaro, R.; Zhang, J.; et al. Introducing Advanced Composites and Hybrid Materials. *Adv. Compos. Hybrid Mater.* **2018**, *1*, 1–5. [CrossRef]

76. Alkunte, S.; Fidan, I.; Naikwadi, V.; Gudavasov, S.; Ali, M.A.; Mahmudov, M.; Hasanov, S.; Cheepu, M. Advancements and Challenges in Additively Manufactured Functionally Graded Materials: A Comprehensive Review. *J. Manuf. Mater. Process.* **2024**, *8*, 23. [CrossRef]
77. Doddamani, S.; Kulkarni, S.M.; Joladarashi, S.; TS, M.K.; Gurjar, A.K. Analysis of Light Weight Natural Fiber Composites against Ballistic Impact: A Review. *Int. J. Lightweight Mater. Manuf.* **2023**, *6*, 81–96. [CrossRef]
78. Narayana, K.J.; Burela, R.G. A Review of Recent Research on Multifunctional Composite Materials and Structures with Their Applications. *Mater. Today Proc.* **2018**, *5*, 5580–5590. [CrossRef]
79. González, C.; Vilatela, J.J.; Molina-Aldareguía, J.M.; Lopes, C.S.; LLorca, J. Structural Composites for Multifunctional Applications: Current Challenges and Future Trends. *Prog. Mater. Sci.* **2017**, *89*, 194–251. [CrossRef]
80. Bhatnagar, A. (Ed.) *Lightweight Ballistic Composites: Military and Law-Enforcement Applications*; Woodhead Publishing: Cambridge, UK, 2016. [CrossRef]
81. Abtew, M.A.; Boussu, F.; Bruniaux, P.; Hong, Y. Dynamic Impact Surface Damage Analysis of 3D Woven Para-Aramid Armour Panels Using NDI Technique. *Polymers* **2021**, *13*, 877. [CrossRef]
82. Tsirogiannis, E.C.; Daskalakis, E.; Vogiatzis, C.; Psarommatis, F.; Bartolo, P. Advanced Composite Armor Protection Systems for Military Vehicles: Design Methodology, Ballistic Testing, and Comparison. *Compos. Sci. Technol.* **2024**, *251*, 110486. [CrossRef]
83. Wang, Z.; Yang, L.; Yang, S.; Liu, P.; Wu, L. A Novel Composite Material of Aramid Fiber-Reinforced Polyurea Elastomer Matrix: Mechanical Properties and Ballistic Performance. *Compos. Sci. Technol.* **2025**, *271*, 111370. [CrossRef]
84. Zou, W. Recent Advancements in Ballistic Protection—A Review. *J. Stud. Res.* **2024**, *13*, 5936. [CrossRef]
85. Omerogullari Basyigit, Z. Functional Finishing for Textiles. In *Researches in Science and Art in 21st Century Turkey*; Gece Publishing: Ankara, Turkey, 2017; pp. 2297–2308.
86. Abtew, M.A.; Boussu, F.; Bruniaux, P. Dynamic Impact Protective Body Armour: A Comprehensive Appraisal on Panel Engineering Design and Its Prospective Materials. *Def. Technol.* **2021**, *17*, 2027–2049. [CrossRef]
87. Sadiku, R.; Agboola, O.; Mochane, M.; Fasiku, V.; Owonubi, S.; Ibrahim, I.; Abbavaram, B.; Kupolati, W.; Jayaramudu, T.; Uwa, C.; et al. The Use of Polymer Nanocomposites in the Aerospace and the Military/Defence Industries. In *Handbook of Research on Polymer Nanocomposites for Advanced Engineering and Military Applications*; IGI Global: Hershey, PA, USA, 2021; pp. 306–332. [CrossRef]
88. Musa, A.A.; Bello, A.; Adams, S.M.; Onwualu, A.P.; Anye, V.C.; Bello, K.A.; Obianyo, I.I. Nano-Enhanced Polymer Composite Materials: A Review of Current Advancements and Challenges. *Polymers* **2025**, *17*, 893. [CrossRef] [PubMed]
89. Wu, S.; Sikdar, P.; Bhat, G.S. Recent Progress in Developing Ballistic and Anti-Impact Materials: Nanotechnology and Main Approaches. *Def. Technol.* **2023**, *21*, 33–61. [CrossRef]
90. Arulvel, S.; Reddy, D.M.; Rufuss, D.D.W.; Akinaga, T. A Comprehensive Review on Mechanical and Surface Characteristics of Composites Reinforced with Coated Fibres. *Surf. Interfaces* **2021**, *27*, 101449. [CrossRef]
91. Bhanuprakash, L.; Parasuram, S.; Varghese, S. Experimental Investigation on Graphene Oxides Coated Carbon Fibre/Epoxy Hybrid Composites: Mechanical and Electrical Properties. *Compos. Sci. Technol.* **2019**, *179*, 134–144. [CrossRef]
92. Riahi, S.; Nemati, A.; Khodabandeh, A.R.; Baghshahi, S. Investigation of Interfacial and Mechanical Properties of Alumina-Coated Steel Fiber Reinforced Geopolymer Composites. *Constr. Build. Mater.* **2021**, *288*, 123118. [CrossRef]
93. Hu, C.; Liao, X.; Qin, Q.H.; Wang, G. The Fabrication and Characterization of High Density Polyethylene Composites Reinforced by Carbon Nanotube Coated Carbon Fibers. *Compos. Part A Appl. Sci. Manuf.* **2019**, *121*, 149–156. [CrossRef]
94. Pillai, R.; Jariwala, C.; Kumar, K.; Kumar, S. Process Optimisation of SiO_2 Interface Coating on Carbon Fibre by RF PECVD for Advanced Composites. *Surf. Interfaces* **2017**, *9*, 21–27. [CrossRef]
95. Zhao, G.; Liu, H.Y.; Du, X.; Zhou, H.; Mai, Y.W.; Jia, Y.Y.; Yan, W. Glass Fibres Coated with Flame Synthesised Carbon Nanotubes to Enhance Interface Properties. *Compos. Commun.* **2021**, *24*, 100623. [CrossRef]
96. Nurazzi, N.M.; Asyraf, M.R.; Khalina, A.; Abdullah, N.; Aisyah, H.A.; Rafiqah, S.A.; Sabaruddin, F.A.; Kamarudin, S.H.; Norrrahim, M.N.; Ilyas, R.A.; et al. A Review on Natural Fiber Reinforced Polymer Composite for Bullet Proof and Ballistic Applications. *Polymers* **2021**, *13*, 646. [CrossRef] [PubMed]
97. Pierre, A.C. Gelation. In *Introduction to Sol-Gel Processing*; Pierre, A.C., Ed.; Springer: Boston, MA, USA, 1998; pp. 169–204. [CrossRef]
98. Hench, L.L.; West, J.K. The Sol-Gel Process. *Chem. Rev.* **1990**, *90*, 33–72. [CrossRef]
99. Wang, D.; Bierwagen, G.P. Sol–Gel Coatings on Metals for Corrosion Protection. *Prog. Org. Coat.* **2009**, *64*, 327–338. [CrossRef]
100. Dimitriev, Y.; Ivanova, Y.; Iordanova, R. History of Sol-Gel Science and Technology. *J. Univ. Chem. Technol. Metall.* **2008**, *43*, 181–192.
101. Wright, J.D.; Sommerdijk, N.A. *Sol-Gel Materials: Chemistry and Applications*; CRC Press: Singapore, 2000; Volume 4. [CrossRef]
102. Liu, X.; Yu, W.; Xu, P. Improving the Photo-Stability of High Performance Aramid Fibers by Sol-Gel Treatment. *Fibers Polym.* **2008**, *9*, 455–460. [CrossRef]

103. Brzeziński, S.; Kowalczyk, D.; Borak, B.; Jasiorski, M.; Tracz, A. Applying the Sol-Gel Method to the Deposition of Nanocoats on Textiles to Improve Their Abrasion Resistance. *J. Appl. Polym. Sci.* **2012**, *125*, 3058–3067. [CrossRef]
104. Schramm, C.; Rinderer, B. Dyeing and DP Treatment of Sol-Gel Pre-Treated Cotton Fabrics. *Fibers Polym.* **2011**, *12*, 226–232. [CrossRef]
105. Chu, Y.; Chen, X.; Wang, Q.; Cui, S. An Investigation on Sol–Gel Treatment to Aramid Yarn to Increase Inter-Yarn Friction. *Appl. Surf. Sci.* **2014**, *320*, 710–717. [CrossRef]
106. Chu, Y.; Rahman, M.R.; Min, S.; Chen, X. Experimental and Numerical Study of Inter-Yarn Friction Affecting Mechanism on Ballistic Performance of Twaron® Fabric. *Mech. Mater.* **2020**, *148*, 103421. [CrossRef]
107. Ceratti, D.R.; Louis, B.; Paquez, X.; Faustini, M.; Grosso, D. A New Dip Coating Method to Obtain Large-Surface Coatings with a Minimum of Solution. *Adv. Mater.* **2015**, *27*, 4958–4962. [CrossRef]
108. Gaulding, E.A.; Diroll, B.T.; Goodwin, E.D.; Vrtis, Z.J.; Kagan, C.R.; Murray, C.B. Deposition of Wafer-Scale Single-Component and Binary Nanocrystal Superlattice Thin Films via Dip-Coating. *Adv. Mater.* **2015**, *27*, 2846–2851. [CrossRef] [PubMed]
109. Dey, M.; Doumenc, F.; Guerrier, B. Numerical Simulation of Dip-Coating in the Evaporative Regime. *Eur. Phys. J. E* **2016**, *39*, 19. [CrossRef]
110. Tseghai, G.B.; Malengier, B.; Fante, K.A.; Nigusse, A.B.; Van Langenhove, L. Development of a Flex and Stretchy Conductive Cotton Fabric via Flat Screen Printing of PEDOT:PSS/PDMS Conductive Polymer Composite. *Sensors* **2020**, *20*, 1742. [CrossRef] [PubMed]
111. Tang, X.; Yan, X. Dip-Coating for Fibrous Materials: Mechanism, Methods and Applications. *J. Sol-Gel Sci. Technol.* **2017**, *81*, 378–404. [CrossRef]
112. Mirmohammadsadeghi, S.; Juhas, D.; Parker, M.; Peranidze, K.; Van Horn, D.A.; Sharma, A.; Patel, D.; Sysoeva, T.A.; Klepov, V.; Reukov, V. The Highly Durable Antibacterial Gel-like Coatings for Textiles. *Gels* **2024**, *10*, 398. [CrossRef]
113. Ghosh, J.; Rupanty, N.S.; Noor, T.; Asif, T.R.; Islam, T.; Reukov, V. Functional Coatings for Textiles: Advancements in Flame Resistance, Antimicrobial Defense, and Self-Cleaning Performance. *RSC Adv.* **2025**, *15*, 10984–11022. [CrossRef]
114. Mattox, D.M. *Handbook of Physical Vapor Deposition (PVD) Processing: Film Formation, Adhesion, Surface Preparation and Contamination Control*; Knovel: Norwich, NY, USA, 1998.
115. Baptista, A.; Silva, F.; Porteiro, J.; Míguez, J.; Pinto, G. Sputtering Physical Vapour Deposition (PVD) Coatings: A Critical Review on Process Improvement and Market Trend Demands. *Coatings* **2018**, *8*, 402. [CrossRef]
116. Das, S.; Kumar, S.; Samal, S.K.; Mohanty, S.; Nayak, S.K. A Review on Superhydrophobic Polymer Nanocoatings: Recent Development and Applications. *Ind. Eng. Chem. Res.* **2018**, *57*, 2727–2745. [CrossRef]
117. Muñoz, R.; Gómez-Aleixandre, C. Review of CVD Synthesis of Graphene. *Chem. Vap. Depos.* **2013**, *19*, 297–322. [CrossRef]
118. Pierson, H.O. Fundamentals of Chemical Vapor Deposition. In *Handbook of Chemical Vapor Deposition: Principles, Technology, and Applications*, 2nd ed.; Materials Science and Process Technology Series; Noyes Publications: Saddle River, NJ, USA, 1999; pp. 36–67.
119. Lamm, B.W.; Mitchell, D.J. Chemical Vapor Deposition of Zirconium Compounds: A Review. *Coatings* **2023**, *13*, 266. [CrossRef]
120. Pierson, H.O. CVD Processes and Equipment. In *Handbook of Chemical Vapor Deposition: Principles, Technology, and Applications*, 2nd ed.; Materials Science and Process Technology Series; Noyes Publications: Saddle River, NJ, USA, 1999; pp. 108–146.
121. Xu, Y.; Yan, X.-T. Chemical Vapor Deposition Systems Design. In *Chemical Vapour Deposition; Engineering Materials and Processes*; Springer: London, UK, 2010; pp. 73–128. [CrossRef]
122. Martinu, L.; Zabeida, O.; Klemberg-Sapieha, J.E. Plasma-Enhanced Chemical Vapor Deposition of Functional Coatings. In *Handbook of Deposition Technologies for Films and Coatings*; Martin, P.M., Ed.; Elsevier: Amsterdam, The Netherlands, 2010; pp. 392–465.
123. Walton, S.G.; Greene, J.E. Plasmas in Deposition Processes. In *Handbook of Deposition Technologies for Films and Coatings*; Martin, P.M., Ed.; Elsevier: Amsterdam, The Netherlands, 2010; pp. 32–92.
124. Struszczyk, M.; Puszkarz, A.; Wilbik-Hałgas, B.; Cichecka, M.; Litwa, P.; Urbaniak-Domagała, W.; Krucinska, I. The Surface Modification of Ballistic Textiles Using Plasma-Assisted Chemical Vapor Deposition (PACVD). *Text. Res. J.* **2014**, *84*, 2085–2093. [CrossRef]
125. Struszczyk, M.H.; Puszkarz, A.K.; Miklas, M.; Wilbik-Hałgas, B.; Cichecka, M.; Urbaniak-Domagała, W.; Krucińska, I. Effect of Accelerated Ageing on Ballistic Textiles Modified by Plasma-Assisted Chemical Vapour Deposition (PACVD). *Fibres Text. East. Eur.* **2016**, *24*, 83–88. [CrossRef]
126. Łandwijt, M.; Struszczyk, M.H.; Urbaniak-Domagała, W.; Puszkarz, A.K.; Wilbik-Hałgas, B.; Cichecka, M.; Krucińska, I. Ballistic Behaviour of PACVD-Modified Textiles. *Fibres Text. East. Eur.* **2019**, *27*, 85–90. [CrossRef]
127. Struszczyk, M.H.; Urbaniak-Domagała, W.; Puszkarz, A.K.; Wilbik-Hałgas, B.; Cichecka, M.; Sztajnowski, S.; Puchalski, M.; Miklas, M.; Krucińska, I. Structural Changes in the PACVD-Modified Para-Aramid Ballistic Textiles during the Accelerated Ageing. *Fibres Text. East. Eur.* **2017**, *25*, 36–41. [CrossRef]

128. Bishop, J.E.; Routledge, T.J.; Lidzey, D.G. Advances in Spray-Cast Perovskite Solar Cells. *J. Phys. Chem. Lett.* **2018**, *9*, 1977–1984. [CrossRef]
129. Gittens, G.J. Variation of Surface Tension of Water with Temperature. *J. Colloid Interface Sci.* **1969**, *30*, 406–412. [CrossRef]
130. Patel, M.; Baishya, H.; Gupta, R.; Garai, R.; Iyer, P. Thin Film Solution Processable Perovskite Solar Cell. In *Perovskite Materials, Devices and Integration*; IntechOpen: London, UK, 2022. [CrossRef]
131. Rubin, W.; Zhai, W.; Li, F.; Li, Y.; Zhang, W.; Liang, Y.; Dong, B.; Wang, X. Enhancing Stab Resistance of Thermoset–Aramid Composite Fabrics by Coating with SiC Particles. *J. Ind. Text.* **2019**, *48*, 152808371876080. [CrossRef]
132. Vignesh, S.; Surendran, R.; Sekar, T.; Rajeswari, B. Ballistic Impact Analysis of Graphene Nanosheets Reinforced Kevlar-29. *Mater. Today Proc.* **2021**, *45*, 788–793. [CrossRef]
133. Pandya, K.S.; Naik, N.K. Analytical and Experimental Studies on Ballistic Impact Behavior of Carbon Nanotube Dispersed Resin. *Int. J. Impact Eng.* **2015**, *76*, 49–59. [CrossRef]
134. Dixit, P.; Ghosh, A.; Majumdar, A. Hybrid Approach for Augmenting the Impact Resistance of P-Aramid Fabrics: Grafting of ZnO Nanorods and Impregnation of Shear Thickening Fluid. *J. Mater. Sci.* **2019**, *54*, 13106–13117. [CrossRef]
135. Rahman, A.S.; Mathur, V.; Asmatulu, R. Effect of Nanoclay and Graphene Inclusions on the Low-Velocity Impact Resistance of Kevlar-Epoxy Laminated Composites. *Compos. Struct.* **2018**, *187*, 481–488. [CrossRef]
136. Markusík, D.; Bocian, L.; Novotný, R.; Palovčík, J.; Hrbáčová, M. Influence of Fumed Nanosilica on Ballistic Performance of UHPCs. *Materials* **2023**, *16*, 2151. [CrossRef] [PubMed]
137. Feng, X.; Li, S.; Wang, Y.; Wang, Y.; Liu, J. Effects of Different Silica Particles on Quasi-Static Stab Resistant Properties of Fabrics Impregnated with Shear Thickening Fluids. *Mater. Des.* **2014**, *64*, 456–461. [CrossRef]
138. Obradović, V.; Stojanović, D.; Jancic Heinemann, R.; Zivkovic, I.; Radojevic, V.; Uskokovic, P.; Aleksic, R. Ballistic Properties of Hybrid Thermoplastic Composites with Silica Nanoparticles. *J. Eng. Fibers Fabr.* **2014**, *9*, 1914. [CrossRef]
139. Gunes, C.; Yildiz, S.; Güneş, M.; Senel, F.; Tanoglu, M. Stab and Ballistic Performances of Aramid Fabrics Impregnated with Silica Based Shear Thickening Fluids. *Ömer Halisdemir Univ. J. Eng. Sci.* **2021**, *10*, 847–854. [CrossRef]
140. Tian, H.; Zhang, B. Nano-Projectiles Impact on Graphene/SiC Laminates. *Appl. Surf. Sci.* **2022**, *591*, 153113. [CrossRef]
141. Lee, J.-H.; Loya, P.E.; Lou, J.; Thomas, E.L. Dynamic Mechanical Behavior of Multilayer Graphene via Supersonic Projectile Penetration. *Science* **2014**, *346*, 1092–1096. [CrossRef]
142. Novoselov, K.S.; Fal'ko, V.I.; Colombo, L.; Gellert, P.R.; Schwab, M.G.; Kim, K. A Roadmap for Graphene. *Nature* **2012**, *490*, 192–200. [CrossRef]
143. Bhuyan, M.S.A.; Uddin, M.N.; Islam, M.M.; Bipasha, F.A.; Hossain, S.S. Synthesis of Graphene. *Int. Nano Lett.* **2016**, *6*, 65–83. [CrossRef]
144. Verma, G.; Goel, R.; Kaur, N.; Singh, M.K.; Rangappa, S.M.; Siengchin, S. Understanding Behaviour of Graphene in Natural Fibre Composites: A Comprehensive Review. *Eur. Polym. J.* **2025**, *232*, 113959. [CrossRef]
145. Bizao, R.A.; Machado, L.D.; de Sousa, J.M.; Pugno, N.M.; Galvao, D.S. Scale Effects on the Ballistic Penetration of Graphene Sheets. *Sci. Rep.* **2018**, *8*, 6750. [CrossRef] [PubMed]
146. Pugno, N.M.; Coluci, V.R.; Galvao, D.S. Nanotube- or Graphene-Based Nanoarmors. In *Computational & Experimental Analysis of Damaged Materials*; Pavlou, D.G., Ed.; Transworld Research Network: Kerala, India, 2007; pp. 145–154.
147. Dewapriya, M.A.N.; Meguid, S.A. Comprehensive Molecular Dynamics Studies of the Ballistic Resistance of Multilayer Graphene-Polymer Composite. *Comput. Mater. Sci.* **2019**, *170*, 109171. [CrossRef]
148. Khine, Y.Y.; Wen, X.; Jin, X.; Foller, T.; Joshi, R. Functional Groups in Graphene Oxide. *Phys. Chem. Chem. Phys.* **2022**, *24*, 26337–26355. [CrossRef]
149. Yu, W.; Sisi, L.; Haiyan, Y.; Jie, L. Progress in the Functional Modification of Graphene/Graphene Oxide: A Review. *RSC Adv.* **2020**, *10*, 15328–15345. [CrossRef]
150. Khan, M.B.; Parvaz, M.; Khan, Z.H. Graphene Oxide: Synthesis and Characterization. In *Advanced Structured Materials*; Springer: Singapore, 2017; Volume 83. [CrossRef]
151. Loudiki, A.; Matrouf, M.; Azriouil, M.; Laghrib, F.; Farahi, A.; Bakasse, M.; Lahrich, S.; El Mhammedi, M.A. Graphene Oxide Synthesized from Zinc-Carbon Battery Waste Using a New Oxidation Process Assisted Sonication: Electrochemical Properties. *Mater. Chem. Phys.* **2022**, *275*, 125308. [CrossRef]
152. da Silva, A.O.; Weber, R.P.; Monteiro, S.N.; Lima, A.M.; Faria, G.S.; da Silva, W.O.; Oliveira, S.S.A.; Monsores, K.G.C.; Pinheiro, W.A. Effect of Graphene Oxide Coating on the Ballistic Performance of Aramid Fabric. *J. Mater. Res. Technol.* **2020**, *9*, 2267–2278. [CrossRef]
153. Kukle, S.; Valisevskis, A.; Briedis, U.; Balgale, I.; Bake, I. Hybrid Soft Ballistic Panel Packages with Integrated Graphene-Modified Para-Aramid Fabric Layers in Combinations with the Different Ballistic Kevlar Textiles. *Polymers* **2024**, *16*, 2106. [CrossRef]
154. Costa, U.O.; Nascimento, L.; Garcia, J.; Monteiro, S.N.; Luz, F.; Pinheiro, W.; Garcia Filho, F.C. Effect of Graphene Oxide Coating on Natural Fiber Composite for Multilayered Ballistic Armor. *Polymers* **2019**, *11*, 1356. [CrossRef]

155. Bidhendi, M.R.T.; Behdinan, K. Graphene Oxide Coated Silicon Carbide Films under Projectile Impacts. *Int. J. Mech. Sci.* **2024**, *261*, 108662. [CrossRef]
156. Lin, G.; Zhou, T.; Zhou, Z.; Sun, W. Laser Induced Graphene for EMI Shielding and Ballistic Impact Damage Detection in Basalt Fiber Reinforced Composites. *Compos. Sci. Technol.* **2023**, *242*, 110182. [CrossRef]
157. Steinke, K.; Groo, L.; Sodano, H.A. Laser Induced Graphene for In-Situ Ballistic Impact Damage and Delamination Detection in Aramid Fiber Reinforced Composites. *Compos. Sci. Technol.* **2021**, *202*, 108551. [CrossRef]
158. Aliana-Cervera, G.; Mattia, D.; Pasquino, C.; Veness, R.; Lunt, A.J.G. Carbon Nanotube Wires for Accelerator Applications. *Mater. Des.* **2025**, *258*, 114606. [CrossRef]
159. Rani, M.; Sehrawat, M.; Sharma, S.; Bharadwaj, S.; Chauhan, G.S.; Dhakate, S.R.; Singh, B.P. Carbon Nanotube-Based Soft Body Armor: Advancements, Integration Strategies, and Future Prospects. *Diam. Relat. Mater.* **2024**, *148*, 111446. [CrossRef]
160. Li, D.; Wang, R.; Liu, X.; Fang, S.; Sun, Y. Shear-Thickening Fluid Using Oxygen-Plasma-Modified Multi-Walled Carbon Nanotubes to Improve the Quasi-Static Stab Resistance of Kevlar Fabrics. *Polymers* **2018**, *10*, 1356. [CrossRef]
161. Micheli, D.; Vricella, A.; Pastore, R.; Delfini, A.; Giusti, A.; Albano, M.; Marchetti, M.; Moglie, F.; Primiani, V.M. Ballistic and Electromagnetic Shielding Behaviour of Multifunctional Kevlar Fiber Reinforced Epoxy Composites Modified by Carbon Nanotubes. *Carbon* **2016**, *104*, 141–156. [CrossRef]
162. Wang, S.; Gao, E.; Xu, Z. Interfacial Failure Boosts Mechanical Energy Dissipation in Carbon Nanotube Films under Ballistic Impact. *Carbon* **2019**, *146*, 139–146. [CrossRef]
163. Wan Hanif, W.Y.; Risby, M.S.; Noor, M.M. Influence of Carbon Nanotube Inclusion on the Fracture Toughness and Ballistic Resistance of Twaron/Epoxy Composite Panels. *Procedia Eng.* **2015**, *114*, 118–123. [CrossRef]
164. Soorya Prabha, P.; Ragavi, I.G.; Rajesh, R.; Pradeep Kumar, M. FEA Analysis of Ballistic Impact on Carbon Nanotube Bulletproof Vest. *Mater. Today Proc.* **2021**, *46*, 3937–3940. [CrossRef]
165. Tsirogiannis, E.C.; Daskalakis, E.; Hassan, M.H.; Omar, A.M.; Bartolo, P. Ballistic Design and Testing of a Composite Armour Reinforced by CNTs Suitable for Armoured Vehicles. *Def. Technol.* **2024**, *32*, 173–195. [CrossRef]
166. Du, Z.; Xiao, K.; Huang, C.; Wu, X. Dynamic Behavior of Tunable Bouligand-Structured Carbon Nanotube Films under Micro-Ballistic Impact. *Nano Mater. Sci.* **2025**. [CrossRef]
167. Zhang, W.; Xiao, K.; Hu, D.; Huang, C.; Wu, X. Anomalous Size Effect of Impact Resistance in Carbon Nanotube Film. *Mater. Today Adv.* **2024**, *24*, 100528. [CrossRef]
168. Cao, S.; Pang, H.; Zhao, C.; Xuan, S.; Gong, X. The CNT/PSt-EA/Kevlar Composite with Excellent Ballistic Performance. *Compos. Part B Eng.* **2020**, *185*, 107793. [CrossRef]
169. Nakonieczna-Dąbrowska, P.; Wróblewski, R.; Płocińska, M.; Leonowicz, M. Impact of the Carbon Nanofillers Addition on Rheology and Absorption Ability of Composite Shear Thickening Fluids. *Materials* **2020**, *13*, 3870. [CrossRef]
170. LaBarre, E.D.; Calderon-Colon, X.; Morris, M.; Tiffany, J.; Wetzel, E.; Merkle, A.; Trexler, M. Effect of a Carbon Nanotube Coating on Friction and Impact Performance of Kevlar. *J. Mater. Sci.* **2015**, *50*, 5431–5442. [CrossRef]
171. Liu, M.; Zhang, S.; Liu, S.; Cao, S.; Wang, S.; Bai, L.; Sang, M.; Xuan, S.; Jiang, W.; Gong, X. CNT/STF/Kevlar-Based Wearable Electronic Textile with Excellent Anti-Impact and Sensing Performance. *Compos. Part A Appl. Sci. Manuf.* **2019**, *126*, 105612. [CrossRef]
172. Dhiwar, D.; Verma, S.K.; Gupta, N.; Agnihotri, P.K. Augmenting the Fracture Toughness and Structural Health Monitoring Capabilities in Kevlar/Epoxy Composites Using Carbon Nanotubes. *Eng. Fract. Mech.* **2024**, *297*, 109877. [CrossRef]
173. Lu, C.; Li, S.; Lu, X.; Ma, J.; Ma, W.; Wang, X.; Ba, S. Preparation and Characterization of Shear Thickening Fluid/Carbon Nanotubes/Kevlar Composite Materials. *Polym. Compos.* **2024**, *45*, 3146–3155. [CrossRef]
174. Hwang, H.-S.; Malakooti, M.H.; Sodano, H.A. Tailored Interyarn Friction in Aramid Fabrics through Morphology Control of Surface Grown ZnO Nanowires. *Compos. Part A Appl. Sci. Manuf.* **2015**, *76*, 326–333. [CrossRef]
175. Xu, Y.J.; Ma, Y.; Xie, Y.C.; Zhou, Y.; Zhang, H.; Huang, G.Y. Experimental and Numerical Study on the Ballistic Performance of a ZnO-Modified Aramid Fabric. *Int. J. Impact Eng.* **2023**, *175*, 104519. [CrossRef]
176. Chu, Y.; Zhu, B.; Wang, X.; Min, S.; Chen, H.; Huang, W.; Zhang, Y.; Peng, T.; Chen, X. Research on High-Velocity Ballistic Impact of Para-Aramid Sateen Fabric with ZnO Nanorods Oriented to the Development of Soft Body Armor. *Mater. Des.* **2024**, *248*, 113384. [CrossRef]
177. Gowthaman, B.; Srinu, G.; Balaganesan, G. Effects of ZnO Nanowire and Silica Coatings on the Inter-Yarn Friction and Ballistic Properties of Kevlar Fabrics. *Int. J. Impact Eng.* **2023**, *178*, 104637. [CrossRef]
178. Malakooti, M.H.; Hwang, H.-S.; Goulbourne, N.C.; Sodano, H.A. Role of ZnO Nanowire Arrays on the Impact Response of Aramid Fabrics. *Compos. Part B Eng.* **2017**, *127*, 222–231. [CrossRef]
179. Steinke, K.; Sodano, H.A. Improved Inter-Yarn Friction and Ballistic Impact Performance of Zinc Oxide Nanowire Coated Ultra-High Molecular Weight Polyethylene (UHMWPE). *Polymer* **2021**, *231*, 124125. [CrossRef]
180. Bilisik, N.E.; Erdogan, G.; Bilisik, K. Pull-Out Properties of Nano-Processed Para-Aramid Fabric Materials in Soft Ballistic: An Experimental Analysis. *Appl. Sci.* **2025**, *15*, 2260. [CrossRef]

181. Song, Y.; Lan, Z.; Deng, J.; Xu, Z.; Nie, Y.; Chen, Y.; Yang, B.; Hao, H. Enhanced Interfacial Properties of Carbon Nanomaterial–Coated Glass Fiber–Reinforced Epoxy Composite: A Molecular Dynamics Study. *Front. Mater.* **2022**, *8*, 828001. [CrossRef]
182. Gupta, S.; Chang, C.; Anbalagan, A.; Tai, N.-H. Reduced Graphene Oxide/Zinc Oxide Coated Wearable Electrically Conductive Cotton Textile for High Microwave Absorption. *Compos. Sci. Technol.* **2020**, *188*, 107994. [CrossRef]
183. Panth, M.; Cook, B.; Alamri, M.; Ewing, D.; Wilson, A.; Wu, J.Z. Flexible Zinc Oxide Nanowire Array/Graphene Nanohybrid for High-Sensitivity Strain Detection. *ACS Omega* **2020**, *5*, 27359–27367. [CrossRef]
184. Arat, R.; Jia, G.; Plentz, J. Wet Chemical Method for Highly Flexible and Conductive Fabrics for Smart Textile Applications. *J. Text. Inst.* **2023**, *114*, 1–6. [CrossRef]
185. Naghizadeh, A.; Khoramishad, H.; Jalaly, M. Effect of Graphene Oxide–Iron Oxide Hybrid Nanocomposite on the High-Velocity Impact Performance of Kevlar Fabrics Impregnated with Nanosilica/Polyethylene Glycol Shear Thickening Fluid. *J. Mater. Des. Appl.* **2023**, *237*, 1803–1813. [CrossRef]

Disclaimer/Publisher's Note: The statements, opinions and data contained in all publications are solely those of the individual author(s) and contributor(s) and not of MDPI and/or the editor(s). MDPI and/or the editor(s) disclaim responsibility for any injury to people or property resulting from any ideas, methods, instructions or products referred to in the content.